UCID- 18009

Lawrence Livermore Laboratory

TECHNICAL CONCEPT FOR ROCK MECHANICS TESTS, CLIMAX GRANITE, NTS

Joseph R Hearst

February 1979

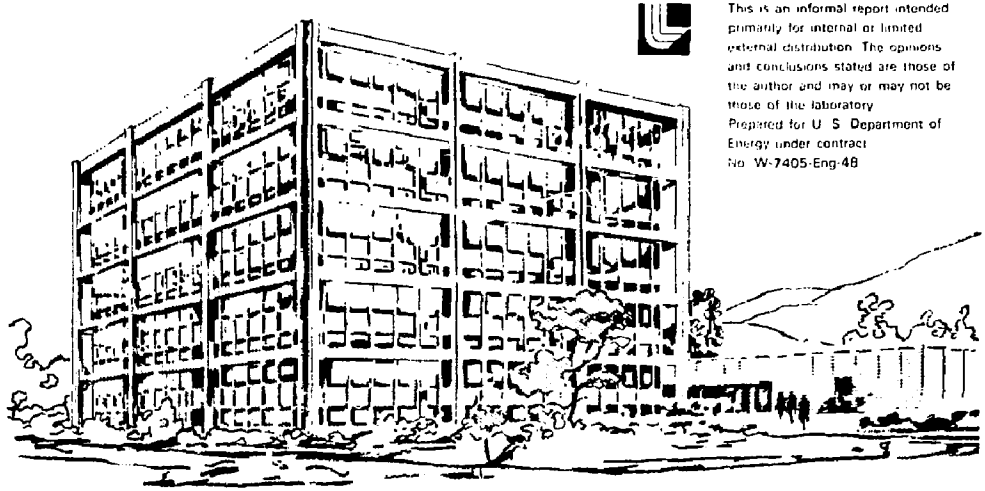

TECHNICAL CONCEPTS OF ROCK MECHANICS TESTS, CLIMAX GRANITE, NTS

Abstract

If we are to believe our predictions of the thermomechanical behavior of the materials surrounding a nuclear waste repository in granite, we must test the computational methods used in making the predictions. If thermal loadings appropriate to a real repository are used, thermally-induced displacements and strains are quite small, and available geotechnical instrumentation is only marginally able to measure these effects to the accuracy desired to make thorough tests of the predictions. We outline a three-step program to address these issues.

1) Conduct experiments in which the thermal loading is large compared to that induced by a real repository. This will permit us to make accurate measurements with available instrumentation.

2) Simultaneously, develop improved instrumentation that will enable us to make accurate measurements of motions induced by thermal loadings appropriate to a real repository.

3) Finally, conduct a second set of experiments, with the improved instrumentation and thermal loading similar to that of a real repository in granite.

If we can predict the effects of this thermal loading to a few percent over distances of tens of meters for time periods of a few years, and demonstrate that these predictions are correct, we can have reasonable confidence that, using the same methods, we can predict the behavior over thousands of meters for hundreds of years to an order of magnitude. That accuracy should be satisfactory for those distances and times.

CONTENTS

Page

PREFACE

An underground repository for high level nuclear waste differs from ordinary underground excavations such as mines or tunnels because it must withstand heat loads as high as 50 watts/m^2 averaged over several Km^2. Local concentrations of heat in storage drifts are greater by a factor of 5 for an excavation ratio of 20%. The highest thermal gradients will exist around the boreholes in which waste canisters are stored; the borehole walls may be as hot as 200°C. The stress field in the undisturbed rock is initially altered by the excavation. Stresses that are imposed due to thermal expansion further modify the in situ stresses. Altering the stress field in a rock mass produces a potential for rock fracture, which may negatively affect the ultimate isolation of the nuclear waste from the biosphere or (in the short term) the retrievability of the waste canisters.

Although there are centuries of experience with underground openings in rock, the thermomechanical stress problem has little precedent, and research programs have been established to study the problem. The Lawrence Livermore Laboratory (LLL) has a program of laboratory and field measurements combined with mathematical modeling. The goal is to understand the effects of thermomechanical stress and to produce a predictive capability for the design of a nuclear waste repository in granitic rock. To date there are three laboratory projects and three field tests, with additional field tests being planned. This report documents some of that planning.

One laboratory project involves the measurement of rock permeability, stress, strain, electrical conductivity and acoustic velocity during a single test loading. These measurements are made through a range of confining pressures, pore (water) pressures, and deviatoric stresses that might exist at depths of up to 2000 m. The basic goal of these measurements is to systematically explore the effects of applied stress on rock permeability of both sound and fractured rock specimens. This will allow us to develop working hypotheses to account for the very low permeabilities of deeply buried rocks. At the same time, systematic data will be developed on the stress-strain relationships and the variation of electrical conductivity and acoustic velocity with applied stress. The former will serve as input to rock mechanics models, and the latter, to the development of remote monitoring techniques.

A second laboratory project involves measuring rock thermal properties as a function of temperature to 500°C and confining pressure to 200 MPa in the presence of pore fluid. Such data are needed for predictive calculations of the effects of waste emplacement. The thermal parameters measured are conductivity, diffusivity, heat capacity, and the linear expansion coefficient.

The relation of the linear thermal expansion coefficient to rock temperature and confining pressure is particularly important for input to calculations of expected stresses resulting from introduction of the thermal load. A third laboratory project is designed to obtain the elastic moduli and Poisson's ratio as functions of temperature, pressure, and pore pressure for use as input to stress calculations.

The three field tests are all located in the Climax granitic stock at the DOE Nevada Test Site. An available vertical shaft provides access to a horizontal drift complex at a depth of 420 m below ground surface. A set of *in situ* thermal properties tests and permeability tests were done in an existing drift in FY 1978. A test of retrievable geologic storage of spent fuel assemblies is under construction, with initial loading of spent fuel scheduled for 1980. Additional rock mechanics tests are being evaluated.

The present report documents some of that evaluation. It does not purport to address all issues necessary to design a waste repository in granitic rock. Issues not addressed, for example, include the question of thermal/radiation induced decrepitation around large boreholes, far-field effects, backfill experiments, predictive capability for permeability changes in the rock, and others.

This report focuses on the issue of validating the predictive capability represented by present rock-mechanics computer codes. In order to do this, we must build calculable experiments and create measurable responses. On the other hand, the experiment must bear on a repository model, so that we must use plausible situations.

Another objective raised in this work is that of examining extreme cases. By overdriving the rock thermally, two independent objectives can be attained: (1) an engineering margin of safety will be established, and (2) the mathematical models used for effects prediction can be validated without waiting for instrumentation refinement and development.

This report, published in an informal LLL series, was an interim progress report on technical concepts for rock mechanics tests needed to produce a predictive capability for the design of a nuclear waste repository in granitic rock. The concepts set forth are being modified as planning progresses, and other issues must be addressed. In issuing a progress report at this time, we have two purposes: (1) to disseminate the ideas set forth in this report, and (2) to receive constructive criticism to aid our planning.

L. D. Ramspott
Leader, Waste Isolation Projects

August, 1979

1.0 INTRODUCTION

This report was prepared for the Nevada Nuclear Waste Storage Program. It analyses possible additions to activities carried out at the Climax granitic stock at the Nevada Test Site (NTS) by the Lawrence Livermore Laboratory (LLL). Initial heater tests which measured in situ thermal properties and permeability were made possible by the availability of existing facilities in the Climax stock, which could be considered a typical granitic rock mass. These tests, in turn, led to the design of a test of the effects of storage of spent reactor fuel in the granitic rock.

The experience with design and operation of these tests led to a number of questions that could not be answered in the Spent Fuel Test. In particular, we wish to know if we can predict the effects of thermal loading appropriate to a real repository by analytical or computer calculations. If we can predict these effects to a few percent over distances of tens of meters for time periods of a few years, and demonstrate that these predictions are correct, we can have reasonable confidence that, using the same methods, we can predict the behavior over thousands of meters for hundreds of years to an order of magnitude. That accuracy should be satisfactory for those distances and times.

2.0 OBJECTIVES

The general objectives of a rock mechanics field program for waste isolation are twofold. The first is to test the ability of the rock mechanics community to predict the effect of mining and heating in a generic situation resembling a repository in strong brittle rocks. Various plausible situations can be tried. The second is the establishment of safety factors by experimentally causing conditions that result in massive rock failure in an in-situ heating test, and testing the ability of the rock mechanics community to predict these failure conditions.

2.1 Build Calculable Experiments

Most available rock mechanics computer programs have a one- or two-dimensional geometry. When a three-dimensional program is available, most calculations used still are two-dimensional for practical reasons. The experiment should be designed to be describable by such a geometry. Two cases are usually available: axisymmetric, where model elements are symmetrical about an axis and the geometry is that of an object of revolution, or planar, where elements are symmetrical about a plane of symmetry, and the geometry is infinite in one (usually horizontal) dimension.

2.2 Use Plausible Situations

The simplest situation is that of a borehole containing a heater. Normally a drift is present, since the emplacement hole must be produced somehow. One can either make the hole so deep that measurements made radially out from the hole are not affected by the drift or take the drift into account in the calculations. A short drift with a single hole can be represented by the axisymmetric case with measurements made radially from its axis. This is conceptually the simplest situation. The planar case is an approximation of a row of closely spaced holes and is more realistic simulation of a real repository. Measurements would be made on a plane intersecting the midpoint of the heaters. In both cases measurements could be made at other elevations, and since the calculations are two-dimensional, we could thus test our ability to predict end effects.

Another useful experiment is that of a drift with a heated floor to simulate the rock openings of a repository heated by a large number of fuel canisters emplaced in them. This permits calculation of the effects of the heat on the walls, floor, and roof without having to be able to deal with buried heaters. The axisymmetric case is a circular room with an arched roof. The planar case, which is more realistic, is an infinitely long drift. It may well be useful to include a pillar in this experiment. A pillar (Figure 1) is defined as the unmined rock between two drifts. Since the calculation assumes the pillar to be infinitely long, some attention must be given to its ends in the real experiment; they can be attached to or detached from the parent rock mass.

2.3 Create Measurable Responses

Preliminary calculations (Section 4.1) indicate that the motions that will occur under realistic repository situations will be too small to measure accurately in great detail (Section 3.1). One would like to determine medium response caused by heating and mining to an accuracy of at least 10% (preferably 1%) of the total measured response, to provide a reliable check on predictions. There are two approaches to this: to increase the heating beyond reasonable repository levels to induce larger motion, or to improve measurement capabilities. Both will be discussed below.

Preliminary measurements at Stripa[1] yield displacements about a factor of 2 to 4 smaller than predicted. This discrepancy is tentatively explained by thermal expansion of the rock into open joints. That is, the displacement is taken up by closure of thin cracks. If expected displacements were an order of magnitude greater than they are in the Stripa experiment, the absolute value of displacement taken up by the cracks would be the same, the fractional effect of cracks would be small, and the measurements, if this explanation is correct, would be comparable in size with the predictions. This is an advantage of causing large motions.

2.4 Examine Extreme Cases

There is no expectation that the roof or walls of a drift or a pillar will fail massively in a realistic brittle-rock repository situation, although local spall or rock bursts may occur. However, in conventional rock mechanics the term "failure" is defined as the point on the stress-strain curve at which strain increases without a corresponding increase in stress. The programs used in prediction of repository behavior generally include failure as defined here, and we should experimentally examine our ability to predict this failure. To do so, we must cause failure.

Experimentally, in a drift or drift and pillar situation, failure is observed as a decrease in stress in the failed rock, and a transfer of the load, (or increased stress) to some other part of the structure. We find that to cause observable failure in a repository situation, we need both unrealistically large heat loads, and an unrealistic geometry in which the underground structure is designed to increase the likelihood of failure.

3.0 CAPABILITIES OF EXISTING GEOTECHNICAL INSTRUMENTATION

In discussing the capabilities of instrumentation, a distinction must be made between sensitivity and accuracy. The sensitivity of an instrument is indicative of the smallest value or increment of the property it measures that can be observed by or read from the instrument; its accuracy is indicative of the degree to which that observed value approaches the true value. For example, an automobile speedometer has a sensitivity of about one kilometer per hour, but its accuracy may be 10-15 KPH, as a policeman may tell the owner. This distinction is particularly important in the application of geotechnical instrumentation to the measurement of the thermomechanical effects caused by heating the rock because measurements are desired near the limits of sensitivity. The instruments are not designed for high temperatures, so their accuracy may decrease markedly as temperature increases. Often they are not designed for long term use, and accuracy may decrease with time as well as temperature.

3.1 Thermocouples

3.1.1 Accuracy

Thermocouples are accurate to at least 1.5°C, which is quite adequate for defining the thermal field. Greater accuracy may be required for temperature correction of other instruments; if so temperature-measuring devices other than thermocouples can be used and will be satisfactory.

3.2 Extensometers

The extensometer is a displacement measuring device. The rod extensometer, with which we are concerned, consists of a rod anchored to the rock at one end at the point whose displacement we wish to measure (Figure 2). The motion of the other end of the rod is measured either with a dial indicator, a micrometer, or a resistive or electromagnetic device fixed to the rock at another point. Ordinarily it is assumed that the length of the rod does not change. Clearly absolute displacement is not measured; only relative displacement of the points in the rock at the anchor and the measuring device.

3.2.1 Sensitivity

The extensometer can be read to 0.025 mm with mechanical equipment and better with resistive or electromagnetic devices. However, on at least one field experiment, it was found that errors of as much as 0.03 mm in 0.5 mm were not unusual, and hysteresis of 0.02 mm was commonly found after a motion of 1.0 mm.[2] Figure 3 shows the errors found in the readout from one extensometer as motions of 2 mm were induced in it.

3.2.2 Temperature effects

Even when made of super-Invar, extensometers require significant temperature correction. The thermal expansion of super-Invar is not constant with temperature, nor is the temperature in an extensometer a linear function of its length. It has been found[3] that with a temperature change of only 40°C the coefficient of expansion is large enough to require measurements of temperature as a function of position. Therefore if linear interpolation is used between sparsely measured temperature values along the length of an extensometer, errors of as much as 0.025 mm per metre of rock can be introduced.

3.2.3 Long-term stability

It has been found[4] that over a period of months, super-Invar exhibits creep. Figure 4 shows the result for one formulation, with optimum heat-treating to reduce creep. It can be seen that errors of as much as 0.04 mm in a 10 m rod can be introduced by creep.

3.2.4 Accuracy

With some temperatures on the order of 100°C, even with all the corrections discussed here the RMS error in length of a rod will be at least 0.05 mm, and the errors could be as large as 0.09 mm.

3.3 Vibrating-wire "Stress" Gages

The Creare, or vibrating wire, gage[7] consists essentially of a thick-walled cylinder fitted tightly into a borehole with its axis parallel to the hole (Figure 5). A highly-stressed wire is fitted along a diameter of the cylinder and vibrated at its resonant frequency. This frequency is a function of the length and tension of the wire, thus of the diameter of the cylinder, and thus of the stress across the hole. The usual stress gage is considered a "hard" inclusion; its modulus of elasticity is much greater than that of the rock and therefore its diameter change is proportional to the stress it experiences, and the rock modulus can almost be neglected. In the case of granite, the assumption of a hard inclusion is not really correct. In any case, what is measured is the stress in the rock-gage system, not the free-field stress in the rock itself.

When a material is heated, it expands. If a plate with a hole in it is heated, the hole expands. Contrariwise, when a plate is cooled, it, and a hole in it, contracts. These changes in hole diameter can be treated as strains and a proper thermomechanical calculation will include these strains. They can occur even if there is no stress in the material. They can also be superposed on other stress-induced strains.

If a fairly hard inclusion is placed in a hole in an unstressed medium, and the medium is then heated or cooled, a stress will arise because of the difference in thermal expansion between the inclusion and the hole (in the case of heating, it is assumed that the hole is stressed when the inclusion is inserted and the stress is relieved on heating). If the inclusion is a stress gage, the stress it reads is that caused by its presence, even in the absence of other stresses in the medium.

If a soft inclusion is placed in the hole, it will not cause a stress, but if it is a stress gage its "stress" output will actually be the non-stress-induced strain in the medium.

Therefore it should be recognized that a stress "gage" which measures the change in diameter of a hole in a heated rock is, if soft compared to the rock, a strain gage, and if hard compared to the rock, of questionable interpretability.

3.3.1 Sensitivity

Problems have been found in establishing contact between the gage and the rock. The hole must be reamed to precise roundness for good contact and this is not an easy operation. This seems to be much less of a problem in granite compared to other rocks.

For use in salt the platens, or contact surfaces, between the rock and the gage had to be redesigned before the gage readings became repeatable.[6] It usually works when the hole is contracting; when the hole expands the gage loses contact and falls out unless prestress is very high.

When all of these conditions are satisfied, the gage is said to be precise to about 0.05-0.1 Mpa. Since the gage is actually a strain gage, measuring the diameter of the hole, then using a modulus for granite, the claimed stress sensitivity is equivalent to a strain of about 2×10^{-6}.

3.3.2 Temperature effects

The gage has been found to be stable at high temperature, but elaborate calibrations of each individual gage must be made. In granite it has been found that if a gage is subjected to a stress load cycle there is significant hysteresis.[3] That is, the loading and unloading calibration curves differ, and this difference is of the order of 1 Mpa (20 times the minimum reading). If the gage is then recalibrated at a higher temperature the slope of its calibration curve varies by as much as 40% (Figure 6). If it is then recalibrated at the original temperature, a difference of 10% of the maximum reading is found. It is quite possible that this variation is in fact variation of the rock modulus with temperature. If so, when the same stress state is present in the rock at different temperature, the gage will read different stresses at each temperature.

3.3.3 Accuracy

Presumably both the difference between loading and unloading calibrations, and the variation of calibration with temperature can be understood as gage-rock interaction. It is unlikely that a stress accuracy of better than 1.0 Mpa, or a strain accuracy of 2×10^{-5} can be obtained with existing gages because the gage affects the behavior of the rock (the "hard" gage will prevent the hole from deforming in a normal manner). This behavior is acceptable if the rock modulus is in fact very much less than that of the gage, but this latter assumption is not valid for granite. Detailed knowledge of the rock properties as a function of temperature is required to account for gage-rock interaction.

3.4 Borehole Deformation Gage

The borehole deformation gage, or U.S. Bureau of Mines gage, consists of six cantilevers, each of which bears on a point on the wall of the borehole (Figure 7). Strain gages at the base of each cantilever measure its motion, and thus measure the change in diameter of the hole. This is, by far, the most costly of the gages discussed (at least $1000 per point, without installation).

3.4.1 Sensitivity

A change in diameter of 7.5×10^{-5} mm in a nominal 37.5 mm borehole, corresponding to a strain of 2×10^{-6} is claimed as a least reading.

3.4.2 Temperature Effects

There is a change of calibration factor with temperature.[4] That is, the ratio of voltage to displacement changes with temperature (Figure 8). It is claimed to be linear and repeatable. In addition, there is a voltage offset, different for each gage, that is a function of temperature. Its magnitude is not specified, but it is expressed as a change of voltage as a function of temperature at constant displacement. A third effect is an output voltage generated by the difference in thermal expansion between the rock and the gage.

3.4.3 Accuracy

It is claimed that when the corrections for temperature are all made, diameter changes with a standard deviation of the mean of 1.5×10^{-3} mm can be measured in the 37.5 mm hole.[7] This corresponds to a strain of about 4×10^{-5}. Individual values would have a higher standard deviation than the mean.

3.5 Acoustic Methods

3.5.1 Acoustic Velocity

Acoustic velocity in rock is a function of stress, because cracks close when compressive stress is applied and moduli change with stress. Dilatation, however, can cause cracks to open. Moreover, the time for an acoustic wave to travel between two points will increase drastically if a gas-filled fracture appears between them. Acoustic logs are often used as fracture detectors. Thus, acoustic velocity between transducers placed in two holes a reasonable distance apart can monitor qualitative changes in the rock properties. The method is not generally quantitative with respect to stress or strain, but may aid in understanding other data.

Velocity, attenuation, and waveform of the acoustic signal have been used experimentally as a measure of stress. In the field this technique has been used to measure very small stresses, such as thermal stresses around a power station[8] or earth tides.[9] Field calibration would be needed to ensure accuracy with larger stresses.

These parameters, however, are also strong functions of porosity, saturation, and pore shape.[10] Consequently it may be quite difficult to use this technique as a measure of stress when heat may change saturations and pore shapes.

3.5.2 Acoustic Emission

A technique called acoustic emission uses sensitive transducers to record minute acoustic signals caused by microfracturing or other deformation modes caused by changes in the stress state. This method is less quantitative than acoustic velocity techniques, but may make it feasible to detect fracturing when it occurs, or motion on a fracture, by the stick-slip motion observed at Stripa.[1]

4.0 PRELIMINARY CALCULATIONS

4.1 LLL Calculations

The first predictive calculations made for this program modelled a single spent fuel assembly. The model consisted of a heat source about 4.6 m long, producing 3.67 kW* initially and decaying with time. It was emplaced about 6 m below a drift. No overburden pressure was used. Material properties corresponding to those of intact granite were input. (They will be listed in Section 6.) Maximum horizontal displacements of about 0.5 mm were predicted at 1 yr on the midplane of the heat source. Failure criteria were not included.

4.2 LBL Calculations

Similar calculations had been made by Tin Chan at LBL, to predict rock motions for the Stripa experiments. Similar maximum displacements were predicted.

4.3 Measurability of Motions

In both of these calculations the maximum derivative of displacement with respect to radius (i.e., the strain in an instrument hole) was about 8×10^{-5} at a radius of about 1 m from the heater. As cited above, maximum displacements in the midplane of the heater were about 0.5 mm. At Stripa maximum stress of 30 MPa, corresponding to a free-field strain of 6×10^{-4} was measured with one USBM gage a little over 1 m from a borehole containing a 5 kW heater. Displacements were very small but the results are not understood. At radii greater than 1 m or so from the hole, with 3.7 kW, maximum strains (or stresses) are smaller than or equal to the expected accuracy limits of the instruments. Displacements would be measurable to 10%-20% of the maximum value. In either case, however, changes in strain or displacement as a function of time are too small to measure accurately.

A row of heaters, of course, would produce larger effects but probably still not large enough for measurements of stress/strain vs. time.

4.4 Failure Calculations

Failure, as explained in Section 2.4, is the situation in which the stress peak of the stress-strain curve is reached, and is observed as a reduction of ability of a structural member to carry load. There is no implication of collapse.

---

*Subsequent investigation revealed that the hottest assembly deliverable to NTS in a DOT-licensed cask would be about 2 kW.

Preliminary calculations, in plane geometry, used a model of a pillar 3 m thick and 6 m high.[3] A distributed heat load of kW/m of drift length (the details will be shown in Section 6) in the roof and floor of drifts, caused failure in a few months.

However, it is very difficult to mine such a pillar, and if it were built, its properties would be so dependent on the mining procedure and the preexisting geologic defects in the exposed rock mass that it would be useless as a generic example. A thicker pillar is needed to be less detail dependent.

Calculations with a single room and no pillar indicated that significant failure was not induced under those conditions.

4.5 Conclusions from Preliminary Calculations

4.5.1 Measurability

It appears from the preliminary calculations that an experiment with heating similar to that from a single spent fuel canister cannot produce large enough stress/strain to measure as functions of time with the required accuracy (Section 2.1.4) with available instrumentation. Displacements are marginally measurable.

4.5.2 Failure

It appears that with some modification of the design in the preliminary calculations, failure could be induced in an acceptable pillar, although unrealistically high heat loads will still be required.

5.0 EXPERIMENT OBJECTIVES

From our program objectives and our knowledge of the predicted effects of a model of a spent fuel experiment and our ability to measure them, we can formulate new objectives for the near future.

5.1 Experimental Design

We must design experiments whose effects are large enough to measure to our desired 10% accuracy with equipment available to us at this time. These will include, for example, an experiment similar to that of a single canister in a borehole, but with about five times the normal heat production, and feasible experiments involving heating a pillar for the purpose of inducing failure. This latter experiment can also be used to model the heated tunnel discussed in Section 2.1.2.

5.2 Equipment Improvement

At the same time, we should be improving our measurement ability so that in the future we will be able to measure the "normal" motions induced by spent fuel elements with sufficient accuracy to verify predictions. The disadvantage of the "hotter" experiments proposed above is that rock is nonlinear, and some of the behavior observed will not be completely applicable to the lower heat load of a real repository. Improved instruments, followed by lower-heat experiments, will deal with this problem.

Improved equipment will also require improved calibration capability, and this should not be neglected.

6.0 CALCULATIONS OF POSSIBLE EXPERIMENTS

Three experimental configurations have been simulated: A heater emplaced in a borehole, a heated room, and a heated room containing a pillar. Two programs, the MIT Program ADINA used by LLL, and the RE/SPEC Co. program, SPECTROM II have been used to make these calculations. In one case, both programs calculated a similar configuration as a test.

6.1 Material Properties

6.1.1 Cavity Properties

A large air-filled cavity is a much better thermal "conductor" than a rock mass. This is because not only conduction, but radiation and convection occur, and heat is transferred quite efficiently. Thus, in most of the calculations the tunnel wall was almost an isotherm, wherever the heaters were located.

6.1.2 Rock Properties

Throughout the calculations, the rock was treated as a continuum. The properties used were those of intact granite. Climax Stock material properties were used when they were available, otherwise granite or handbook values were used.

It is of considerable importance that before the experiment is designed in detail, properties of the jointed rock should be obtained and used.

The following properties were used in the LLL and RE/SPEC calculations:

	LLL	RE/SPEC
Thermal Conductivity	2.75 watt/m·K	2.4 watt/m·K
Specific Heat	950 J/kg·K	800 J/kg·K
Poisson's Ratio	0.2	0.2
Coefficient of Thermal Expansion	8×10^{-6}/K	8×10^{-6}/K

Two values of Young's modulus of elasticity were used, 40 GPa and 25 GPa. The latter constant value was used in many RE/SPEC calculations to approximate a decrease in modulus of rock as it is heated.

6.2 LLL Calculations of the Effects of a Heater in a Single Hole

In an axisymmetric calculation, the single hole was modelled with a diameter of 1 m and the heat was placed on the circumference of the hole (the actual design would be a heater on the axis of a large hole). This is the proposed configuration for the experiment because using a larger hole will reduce the temperature at the wall of the hole and thus reduce the possibility of spall or decrepitation. While it may quite desirable to study the spall and joint motion of the borehole, that should be done in a separate experiment. In the calculation the heater was 4 m long, centered 3 m below the floor of the drift, and produced a constant 40 kW, more than an order of magnitude more than expected from a fuel element.

Figure 9 shows displacement as a function of radius on the median plane of the heater for various times. Temperature vs. radius at 48 weeks is also shown. At radii of about 8 m, the temperature rise is well below 100°C and the strain in an instrument hole will be about 3×10^{-4}.

This picture of displacement vs. radius is fairly typical, and leads to an interesting concept of the behavior of an instrument hole in the medium. At first it will contract, as seen from the displacement vs. radius beyond about 4 m. As the heat pulse moves out, the hole will eventually expand in the radial direction, as seen from displacement vs. radius at 1-2 m.

Close in, the strains are as much as 10^{-3} or even greater at early times. But the high temperature will prevent use of instruments this close in.

The planar version of this calculation with an infinite "trench" source, with a heat output of 4 kW per metre of length, gives peak displacements of about 3 mm at a horizontal distance of about 8 m.

6.3 LLL Calculations of a Heated Drift

Figure 10 shows the displacement vs. distance radially from the midplane of a 5 m wide, 5 m high drift heated with floor heaters with uniformly distributed constant heat output of 5 kW/m of drift length. It is the plane strain case. Figure 11 is a similar plot for the displacement vertically above the drift. In this case strains of 2×10^{-4} are seen in the contraction range, and 10^{-3} in expansion. Temperatures are low enough that we should be able to place instruments in the region of expansion.

The axisymmetric calculation is similar, but does not appear to be as useful.

6.4 RE/SPEC Calculations of Heated Drifts and Pillars

RE/SPEC's program includes overburden stress corresponding to a depth of 413 m at a bulk density of 2.7 g/cm. A Mohr-Coulomb failure criterion was used. This criterion states that the maximum shear stress τ_m is determined by

$$\tau_m = S_o + \sigma \tan\phi$$

where S_o is a constant and σ is the mean stress. For these problems the value of ϕ for intact rock was 56° and for failed rock 30°. In all problems but one, S_o was 6.9 MPa for intact rock and 1.7 MPa for failed rock. For one problem (marked "High Strength" in Figure 11) these values of S_o were doubled.

When τ_m is exceeded in a calculation for intact rock, stresses are readjusted so that they correspond to the value of τ_m for failed rock. Thereafter τ_m is not allowed to exceed the value for failed rock. This is the definition of failure in all of these calculations.

The displacements in their heated drift calculation (without overburden) are consistent with those described in Section 6.3 (Figure 12). Their cavity is treated in much the same way as the LLL calculations; the cavity wall is almost an isotherm (Figure 13). Thus, the two calculations are consistent.

6.4.1 In-Rock Heater Calculation with Pillar

Figure 14 shows a sketch of the first RE/SPEC calculation and volumetric averages of stress and temperature rise in the pillar. This is a plane-geometry calculation, with a total load of 8 kW/m, or 4 kW/m in each drift. Thus, it is similar to the LLL calculations except that it treats two drifts. E. Cording[14] contends that when a pillar is heated, its modulus decreases enough that the heating will not develop significant post-peak strength reduction. (Heat-induced stress is much greater than original load.) RE/SPEC used two constant values of modulus (25 and 47 GPa) to investigate this phenomenon. At S_o of 6.9 MPa they calculate failure even at low modulus. (The higher-strength low-modulus problem was not run.)

Figure 15 shows calculated vertical stress at the midplane of the pillar vs. position and time for a problem with a modulus of 25 GPa. Two problems were run, one thermoelastic and one with the Mohr-Coulomb failure criterion. In the problem where the failure criterion is used, it is exceeded in the pillar at 0.3 year and stress in the pillar decreases markedly. This is the indication of "failure". At the same time there is an increase of stress in the walls. At 0.5 yr there is some "failure" in the part of the wall near the room.

Figure 16 shows displacement vs. time at the pillar midplane. Displacement is very great after failure, but even if failure is ignored, the displacements are of the order of 4 mm or so, which are consistent with the LLL calculations.

Figure 17 shows the isotherms for this calculation.

6.4.2 Floor and roof heater calculations

The calculations cited above, with heaters embedded in the rock, are an approximation, in plane strain, of a row of heaters in holes in the floor and ceiling. A situation in which the experiment and calculation can be much more similar is that in which the heaters are distributed uniformly over the floor and roof of the drifts. Heat load is again 8 kW/m. Figures 18 and 19 show stress and displacement at the pillar midplane vs. time and position for this calculation. Displacements are smaller than those with the heaters embedded in the rock, but still large enough to measure. Failure is still predicted. Somewhat larger heat loads may be useful to increase displacements.

Figure 20 shows the isotherms for this calculation.

6.5 Recommended Improvements to Calculations

The graphical output of both LLL and RE/SPEC calculations leaves a great deal to be desired. Much laborious hand plotting must be done to obtain useful output. This graphical output should be improved. Future LLL ADINA calculations should include the overburden and failure capability that is available in the code.

More importantly, the effect of jointing must be modelled more explicitly. SPECTROM-11 is capable of calculating some joint effects. This capability should be introduced into ADINA. Perhaps block-motion codes would be useful here. Dilatation and thermal-stress-induced cracking should be included explicitly. These proposals imply a major code-development program which should be carried on simultaneously with the experimental program described here.

6.6 Future Calculations

6.6.1 Refinement of existing calculations

All of the existing calculations should be redone when more correct values of the physical properties of the granite are available. When a final design of the experiments is complete, of course it should be calculated as well. Failure and known joint structure, in situ horizontal stress, and expected overburden should be included.

7.0 RECOMMENDED FIELD EXPERIMENTS

Two experimental designs are recommended. Each should be replicated at least once, so that we can reduce effects of the specific site chosen for the individual experiment. While we have assumed that the work will be done in the Climax Stock, nothing in the experimental design requires this - the work could be done in many other intrusive bodies.

7.1 Preliminary Measurements

In all cases, an attempt should be made to instrument the experimental areas as early in the mining process as possible. Thus, we will be able to measure the effects of the mining process itself; effects that may be as large as those caused by heating. After the mining is completed and all instruments are installed, they should be operated for a period long enough to assure us that any non-heat-induced measured changes can be accounted for.

7.2 Heater In-Hole Experiment

The results of Figure 9 indicate that the 40 kW heater used in that calculation is more energetic than necessary. The temperatures are too high for the instruments and the displacements larger than really needed. Therefore, a single heater, 4 m long, with 20 kW of power, should provide an adequate experimental situation. The large hole, to reduce the likelihood of spall, should still be used.

A row of holes, with a heat load of 2 kW/m of length is an alternative, but at this time the situation has not been successfully calculated. Furthermore, the axisymmetric case is a better test of the simplest situation, and is recommended.

It would be well to seriously consider increasing the output of the heaters in steps rather than going to 20 kW at once. The steps should be on the order of months in time and perhaps 5 kW in amplitude. There are several advantages to this procedure. It would provide a more stringent test of the calculations, since they must take this time-varying heat load into account. It would make it possible to see if good accuracy in the instruments can be obtained at lower heat loads than these calculations indicate. If so, higher heat loads might be unnecessary. Finally it would reduce further the likelihood of spall at early stages of the experiment.

7.2.1 Instrumentation

Instruments should be placed both in holes drilled down from the drift from which the emplacement hole is drilled, and in horizontal holes drilled from another drift located about 15 m away and below the level of the heater drift. Greenlaw's calculations[11] indicate that a drift at this distance will cause only small perturbations in the displacement. The borehole deformation gages and "stress" gages are best placed in the vertical holes with sensitive axes radial, extensometers in the horizontal ones, although since the calculation is two-dimensional, all kinds of instruments can be profitably placed in both sets of holes. Figure 21 (A-A) is a conceptual sketch of the situation. Joints should be instrumented to monitor motion on them, for example by choosing extensometer anchors on opposite sides of a joint.

7.3 Room and Pillar Experiment

The heated room experiment is needed to make a simple approximation to a real repository tunnel heated from below by waste. The calculations shown in Figures 10-12 give quite measurable deformations at acceptable temperatures. However, the idea that by adding a pillar to the experiment we can cause significant failure with the same heat load is appealing. This is especially true because two consultants strongly disagree as to whether failure will indeed occur.

Therefore, an experiment with two side-by-side drifts, 6 to 9 m wide and 9 m high, separated by a 6 m wide pillar is proposed. It should be heated from the floor to simulate the fairly realistic situation, and a capability of putting 10 kW per m of drift length for 20 m in each drift should be included. A total of 500 kW is now available for the rock mechanics work if done at the 420 m level in the Climax stock; therefore, the two replicate experiments could not proceed at full power simultaneously. However, the recommended power level is 3 or 4 kW per m to start the stepwise heating. The pillar size is chosen to be favorable to failure, not to model reality. The heaters can evidently be made of a material similar or identical to that used in domestic electric ovens.

7.3.1 Instrumentation

The instrumentation for this experiment should again consist of the instruments described in Section 3. In this case, measurements above the drift and radially out from it are desired. Both vertical and horizontal holes are needed to instrument the pillar. These can be made from slant holes drilled from other parts of the drift itself and from an extension of the drift used to emplace the heaters (Section 7.2) in holes. This latter drift will be above the heated drift at the canister position, and can be extended and raised to provide the needed 15-20 m separation from this experiment. (Figure 21, B-B.)

From that extended drift we can drop vertical holes to instrument not only the region above and beside the tunnel, but also the pillar. Instrumentating the rock bolts used in construction of the pillar with load cells and strain gages would also be useful.

Again, joints should be instrumented.

Damage in the walls should be carefully observed, and closure across several diameters of the room should be monitored.

More detailed calculations should be performed to decide whether the ends of the pillars should be free or attached (Figure 1).

7.4 Instrument Details

7.4.1 Thermocouples

Standard thermocouple technology should be adequate.

7.4.2 Extensometers

With displacements on the order of millimeters at temperatures on the order of 100°C, extensometers of ordinary design, but probably made of Super Invar and calibrated as in Sec. 3.2 should be satisfactory. However, we should try some water-cooled extensometers (see Sec. 9.1) in some of the high-temperature areas such as the pillars, and some "breaking-wire" extensometers in the pillars.

7.4.3 Vibrating wire gages

Vibrating wire gages should be satisfactory in the outer parts of the experiments where temperatures are low and the holes contract. A vigorous calibration program in Climax Stock material is required. Deformations in the pillars may be large enough to use these gages even at high temperatures.

7.4.4 Borehole deformation gages

These too should be satisfactory in the outer regions. But their cost precludes using them in large quantities if the vibrating-wire gage becomes equally satisfactory.

7.4.5 Acoustic velocity

Holes should be drilled for velocity-measuring devices, so that they can be tested in this situation. They may give useful data; perhaps they can locate cracked zones in the walls. Acoustic emission should be considered.

7.4.6 Rock bolts

As mentioned above, instrumented rock bolts in the pillars may provide insight into pillar deformation.

7.4.7 Permeability

Hole-to-hole and single hole permeability measurements may be feasible and useful. But since the codes do not predict permeability change, we cannot immediately use such measurements for code verification. Perhaps such predictions will be available in the future, so the measurements are desirable.

7.4.8 Photography

It may be feasible to use borehole photography to detect cracking in walls can also be photographed.

8.0 PHYSICAL PROPERTY MEASUREMENTS

8.1 Field Measurements

It is essential to measure material properties in situ in full-scale geometry. Flatjack tests (Figure 22), in which both the stress and temperature fields in a block surrounded by flatjacks are controlled, are capable of providing stress-strain curves of jointed rock at various temperatures.[15] Blocks 3 m on a side have been successfully studied at stresses up to about 10 MPa. Acoustic velocity, permeability, and resistivity as functions of pressure have also been studied. It should be feasible to determine thermal expansion and thermal conductivity of jointed rock as a function of pressure by this method. A flatjack arrangement can also be used to used to test new geotechnical instruments.

Feedback between the heater experiments and calculations can also serve as a check on in situ properties.

The instrument holes should be cored, allowing a complete description of materials and fractures as a function of position. Careful fracture mapping should also be done in the drifts, pillar surfaces, and heater emplacement holes. Then it will be possible to choose instrument locations with respect to joints and permit instrumentation either of joints or intact rock as desired.

8.2 Laboratory Measurements

It is also necessary to measure thermal expansion coefficients, thermal conductivity, and heat capacity under in situ conditions. This work is in progress at LLL.

We must investigate the effects of thermal stress-induced cracking on the behavior of granite. Literature and laboratory studies will be required.

In situ stress should also be measured in each major block defined by faulting. Then the failure properties should be determined in a stress field corresponding to the in situ stress. This will permit correct values to be input to the calculations.

9.0 INSTRUMENT DEVELOPMENT

The objective cited in Sec. 5.2 is the improvement of instrumentation to make it capable of measuring motions induced by a normal waste canister. Several improved techniques appear possible.

9.1 Cooled Extensometers

By making extensometers out of concentric tubes instead of rods, and circulating water through these tubes, we can probably keep the extensometers at the same temperature throughout their length, rather than having temperature a function of length. Only about a 5 m length of extensometer need be cooled, and this probably no more than 50°C. With good insulation in the hole between the extensometer and the wall, the heat transfer will be on the order of 100 W or less for each set of extensometers close in to the heat source, and proportionately less farther out.

This technique appears sufficiently simple that it may well be field-tested on the experiments proposed above. A proposed design involves the use of metal-rubber bellows tubing to extend the outer extensometer tubes beyond their anchors to provide the water jacket. Ordinary metal, rather than Super-Invar could be used, and thus the water-cooled version would probably be less costly than the current methods.

Careful calibration will still be required, and a calibration capability should be obtained.

9.2 Vibrating-wire Strain Gages

Vibrating-wire strain gages, similar to vibrating-wire stress gages but soft, or of low modulus, compared to the rock instead of hard or of high modulus are commercially available. They are not now designed for emplacement crosswise in a borehole, or for use at high temperature, but it should be feasible to improve their design by paying more attention to thermal properties of materials so that they could be used for this task. Their great virtue is low cost, and the matter is worth pursuing. Emplacement of the gages to measure axial strain (their normal use) may also be useful.

It is especially important that a good calibration facility be provided for this device, so that we can see if medium-dependence can be eliminated or at least corrected for in a consistent fashion.

9.3 High-Temperature Borehole Deformation Gages

It appears possible to build a borehole deformation gage whose physical appearance is quite similar to the gage in Fig. 5, but whose sensors are capacitive or magentic transducers placed under the free ends of the cantilevers rather than strain gages on the fixed ends. This would eliminate the problem of differential expansion of cantilevers and strain gages. Such a device has been built in the past, but did not have good long-term stability.[16]

Now high temperature, very sensitive magnetic displacement transducers are available, good to 0.01 mm or better.[17] (Claims of 10^{-3} mm are made.) While these are very costly, and have not been tested for periods greater than 1000 hr, further testing is warranted and it appears that a good instrument may well be feasible.

9.4 Acoustic Methods

Laboratory and field work has been done to correlate acoustic velocities with stress and fracture in rock. However, in a real situation it is difficult to separate coupling changes from velocity changes. A permanent grouted velocity system is needed to deal with this problem.

Again, calibration in the proper material is required. However, in this case it may be impossible to distinguish among several phenomena that can cause velocity changes. Therefore, considerable thought should be given to the problem before much work is done.

9.5 Holographic Interferometry

The use of holographic interferometry to measure small displacements is a new and promising technique. Methods to use it for measuring small borehole deformations and deformations of pillar walls, especially with infrared mapping of the temperature contours, seem usable in the reasonably near future. Designs for these methods are discussed in the Appendix, which was prepared by Dr. Hartmut Spetzler, an LLL consultant. We must deal with problems of temperature and time stability.

10.0 CONCLUSIONS

The experimental program should consist of three tasks, the first two of which should be carried out simultaneously.

10.1 Task I, Overdriven Field Experiments

We wish to perform experiments that induce motions larger than those expected from a realistic repository situation, up to failure if possible, so that we can test predictive capabilities using currently available measuring equipment. Experiments meeting these criteria are a 20 kW cylindrical heater in a borehole and a pair of tunnels with a pillar in between heated from the floor at about 10 kW/meter.

10.2 Task II, Instrument Development

While the field experiments are in progress, we should field-test water-cooled extensometers. At the same time we should develop improved soft vibrating wire strain gages for insertion across boreholes, and an temperature-insensitive borehole deformation gage if it seems feasible. We should actively pursue holography, since it has the potential to augment all of the gages discussed above.

10.3 Task III, Realistic Field Experiments

Rock is nonlinear, and the properties used to predict Task I may not be entirely applicable to the temperature and stress states in a real repository situation. Therefore, when the field tests in Task I have been completed, and instruments of an order of magnitude better accuracy than are currently available have been developed and calibrated, then the experiments in Task I should be repeated using realistic repository geometry with realistic heat levels. Then we can assure ourselves that we can verify predictions in the range of temperature and stress and therefore the range of rock properties, that is really likely to occur in a repository.

ACKNOWLEDGEMENTS

Many people and organizations contributed to this concept. From RE/SPEC, Inc., Joe Ratigan, Paul Gnirk, and Leo Van Sambeek were major contributors. At Terra Tek, Howard Pratt and Todd Schrauf helped with the original draft and as much with this final draft. Edward Cording at the University of Illinois made a significant contribution, as did Brad Boisen of Terrametrics Co. We wish to thank Tin Chan of the Lawrence Berkeley Laboratory for giving us his calculational results, and Paul Witherspoon for preprints of experimental data.

At LLL, Richard Carlson, Robert Langland, Robert Greenlaw, Harold Ganow, Michael Mayr, Donald Montan, Paul Kasameyer, and Larry Ramspott were among those contributing. Without these people, this report would not be as it is.

REFERENCES

1. Cook, N. G. and Hood, M., Full-Scale and Time Scale Heating Experiments at Stripa; Preliminary Results", Lawrence Berkeley Laboratory Report, to be published.

2. Hood, M., Personal Communication to B. Stromdahl (1978).

3. Pratt, H. R., Hustrulid, W. H., and Simonson, R., Instrumentation Program for Rock Mechanics and Spent Fuel Tests at the Nevada Test Site, Terra-Tek Report TR 78-48 (1978).

4. Marschall, C. W. and Maringer, R. E., "Dimensional Instability", Pergamon Press, Oxford, p. 280.

5. Fossum, A. F., Russell, J. E., and Hansen, F. D., "Analysis of a Vibrating-Wire Stress Gage in Soft Rock", Experimental Mechanics, 7, p. 261 (1977).

6. Ames, E., Personal Communication, Sandia Corporation.

7. Lingle, R., Personal Communication, Terra-Tek.

8. Gladwin, M. T. and Stacey, F. D., "Ultrasonic Pulse Velocity as a Rock Stress Sensor", Tectonophysics, v. 21, p. 39-45 (1974).

9. Bujgum, H., Risbo, T., and Hjortenberg, E., "Precise Continuous Monitoring of Seismic Velocity Variations and Their Possible Connection with Earth Tides", Jour. Geophys. Res., v. 82, p. 5365 (1977).

10. Mavko, G. M. and Nur, A., "Wave Attenuation in Partially Saturated Rocks", Geophysics, v. 44, p. 161 (1979).

11. Greenlaw, R., Personal Communication, Lawrence Livermore Laboratory.

12. Chan, T. and Cook, N., Calculated Thermally-induced Displacements and Stresses for Stripa Heater Experiments, Lawrence Berkeley Laboratory Report, LBL-7061, to be published.

13. Gnirk, P. F., Ratigan, J. L., and Van Sambeek, L. L., Proposed Program Plan for Phase II In Situ Heater Experiments in the Climax Granite, Topical Report RSI-0089, May 23 (1979).

14. Cording, E., Personal Communication, University of Illinois.

15. Pratt, H. R., et al., "Elastic and Transport Properties of an In Situ Joint in Granite", Intl. Journ. Rock Mech. and Min. Sci., v. 14, p. 35 (1977).

16. Boisen, B., Personal Communication, Terrametrics.

17. Phillips, D., Personal Communication, Kaman Scientific.

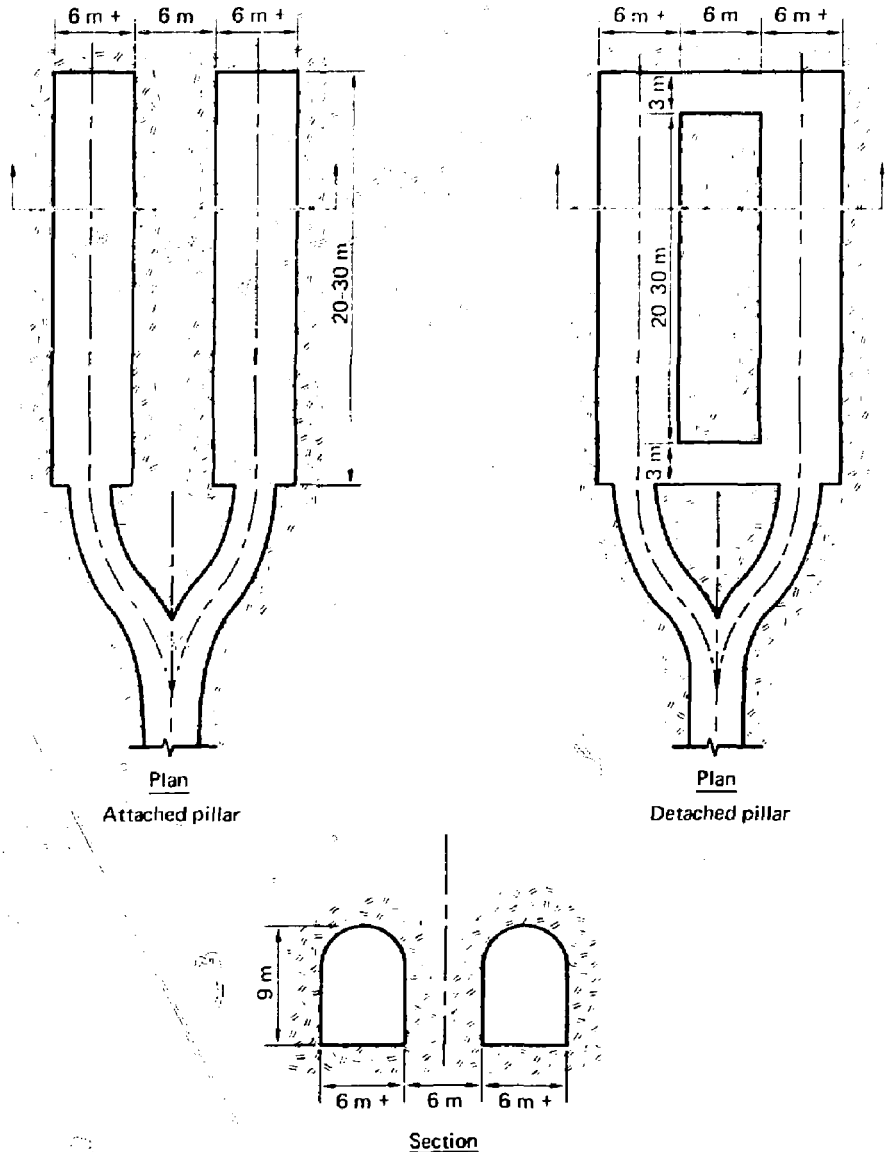

Fig. 1. Illustration of the difference between an attached pillar and a detached pillar.

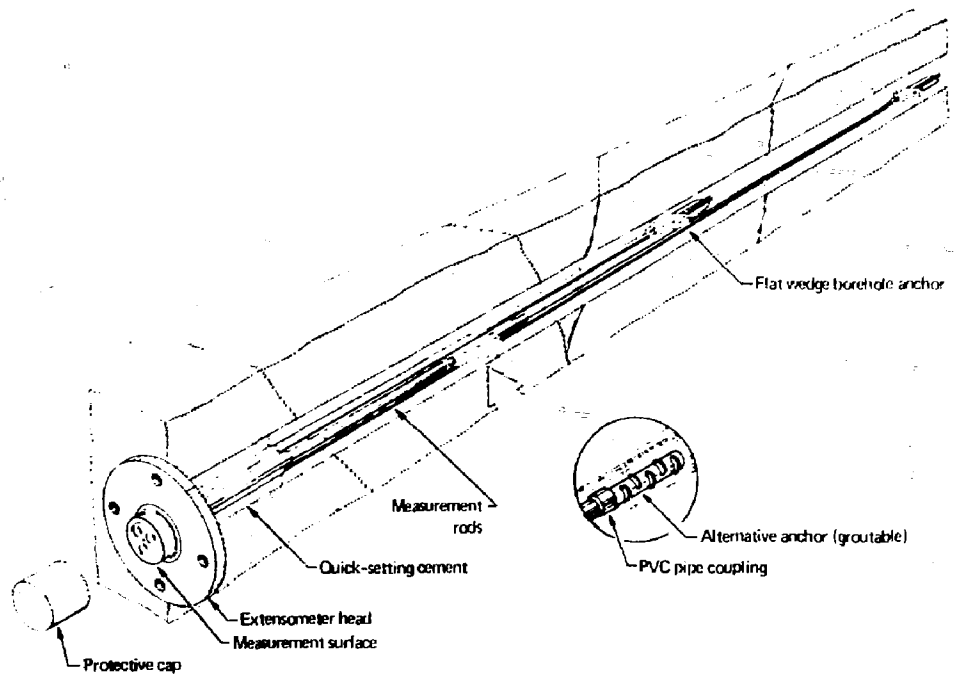

Fig. 2. Illustration of a multiple-point rod extensometer, showing anchors and measuring head.

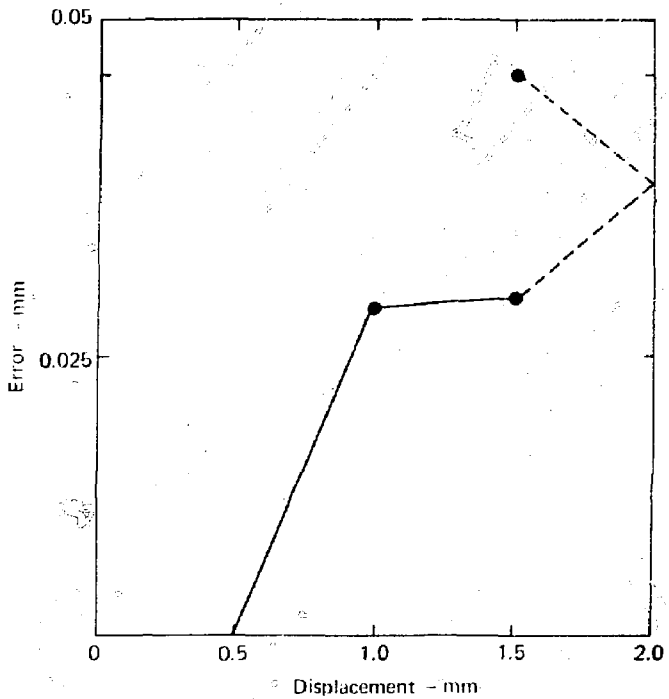

Fig. 3. Error as a function of displacement for a 3-m-long extensometer. This was one of a set of four tested in place in granite at Stripa.[2]

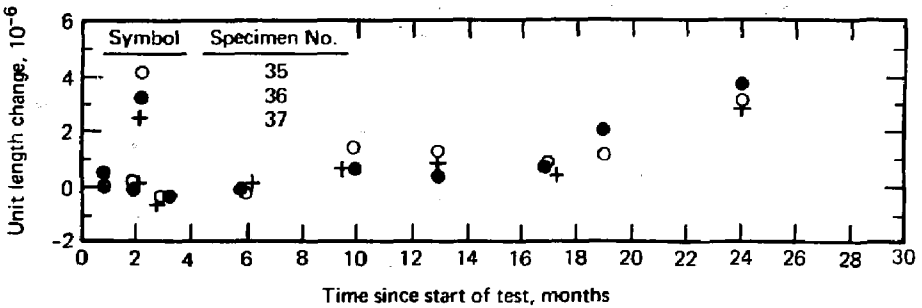

Fig. 4. Change in length as a function of time of a type of super-Invar called Unispan 36. The material was heat-treated to minimize this effect.[4]

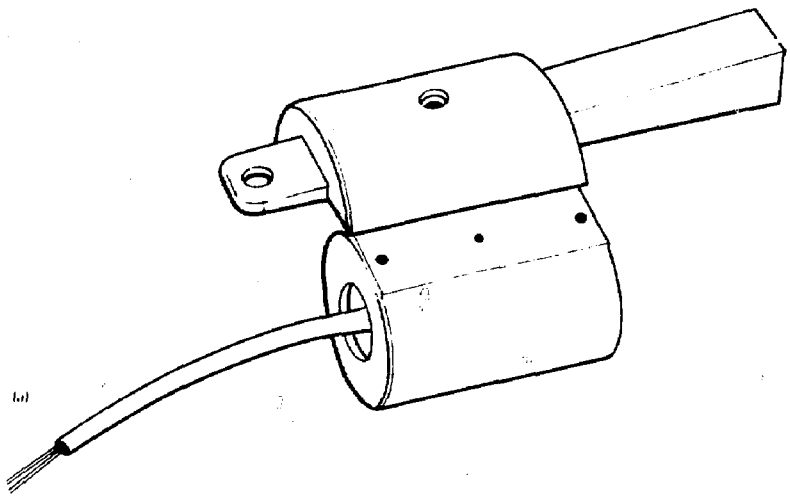

(a)

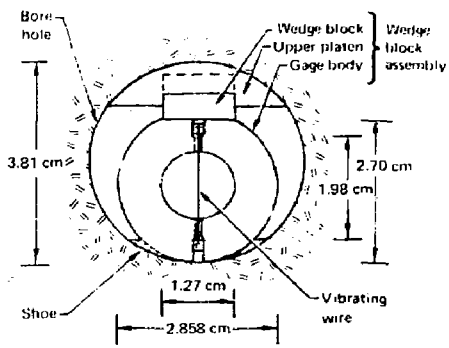

(b) Cross-section view of a vibrating-wire stressmeter transducer in smooth borehole

Fig. 5. Illustration of a vibrating wire stressmeter.

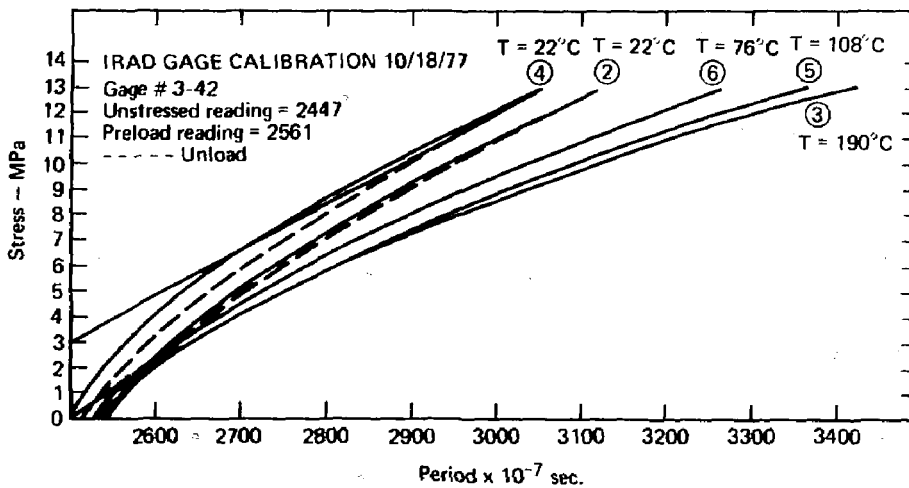

Fig. 6. Typical calibration curves for vibrating wire stressmeters.[3] Numbers illustrate order of measurement.

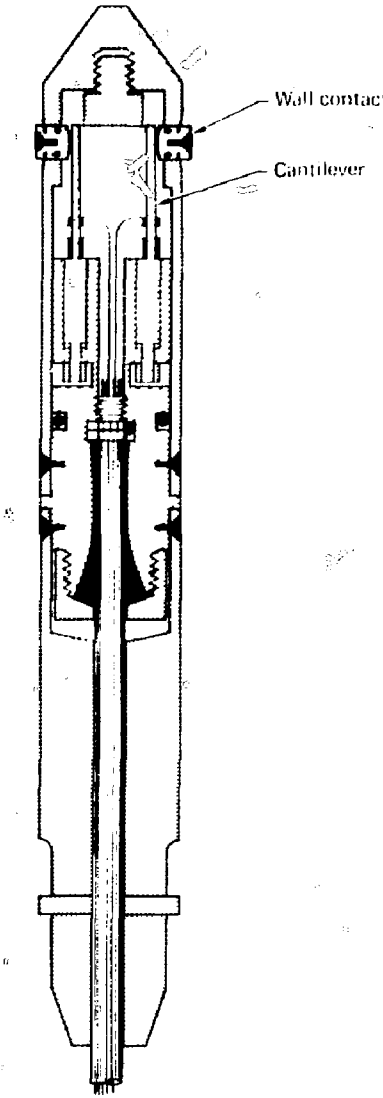

Fig. 7. Illustration of USBM borehole deformation gage.

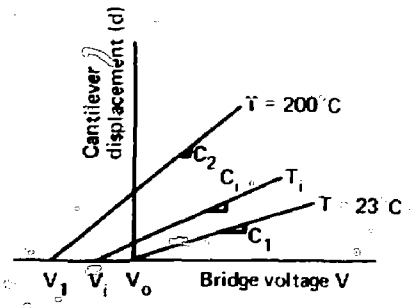

Fig. 8. Calibration curves of USBM borehole deformation gages as a function of temperature[3], T_i is an intermediate temperature.

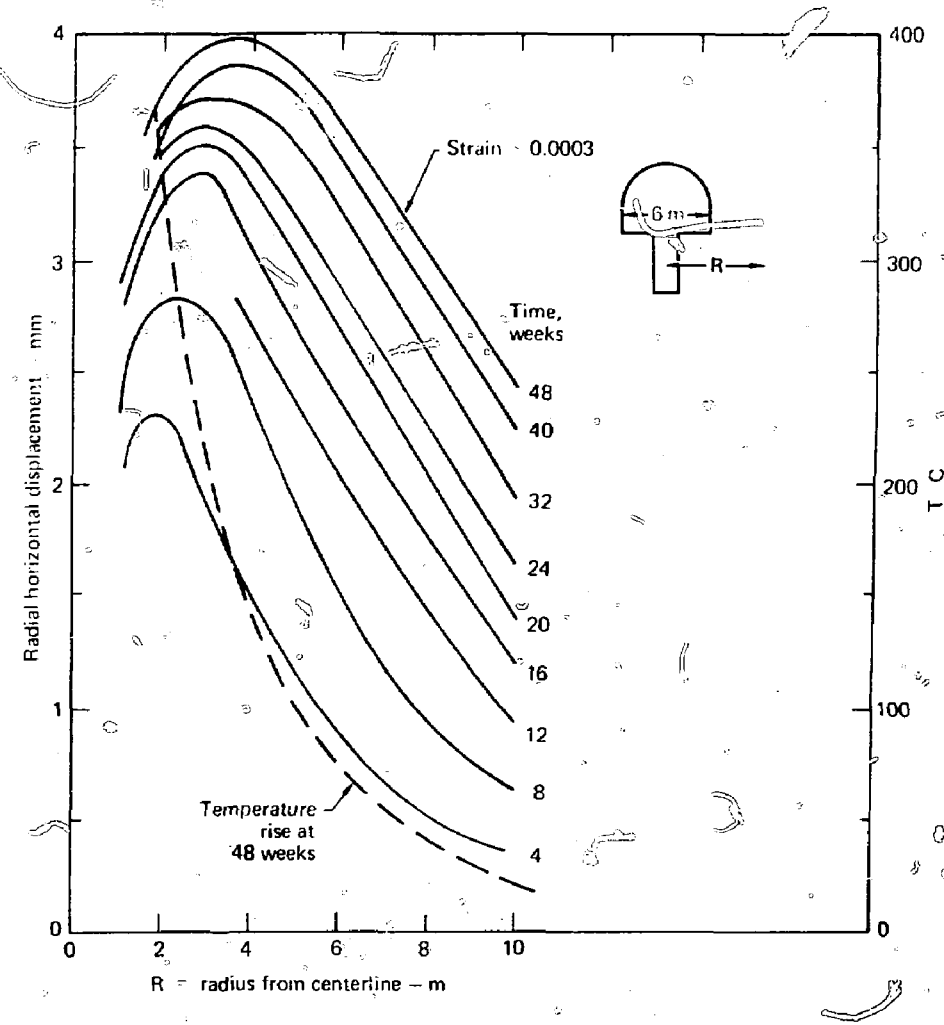

Fig. 9. Calculated radial displacements (positive out) at the center plane of a 1-meter radius hole containing a 40 kw heater. Displacement is shown as a function of radius for several times, and temperature is shown at 48 weeks. Calculation, by LLL, is thermoelastic.

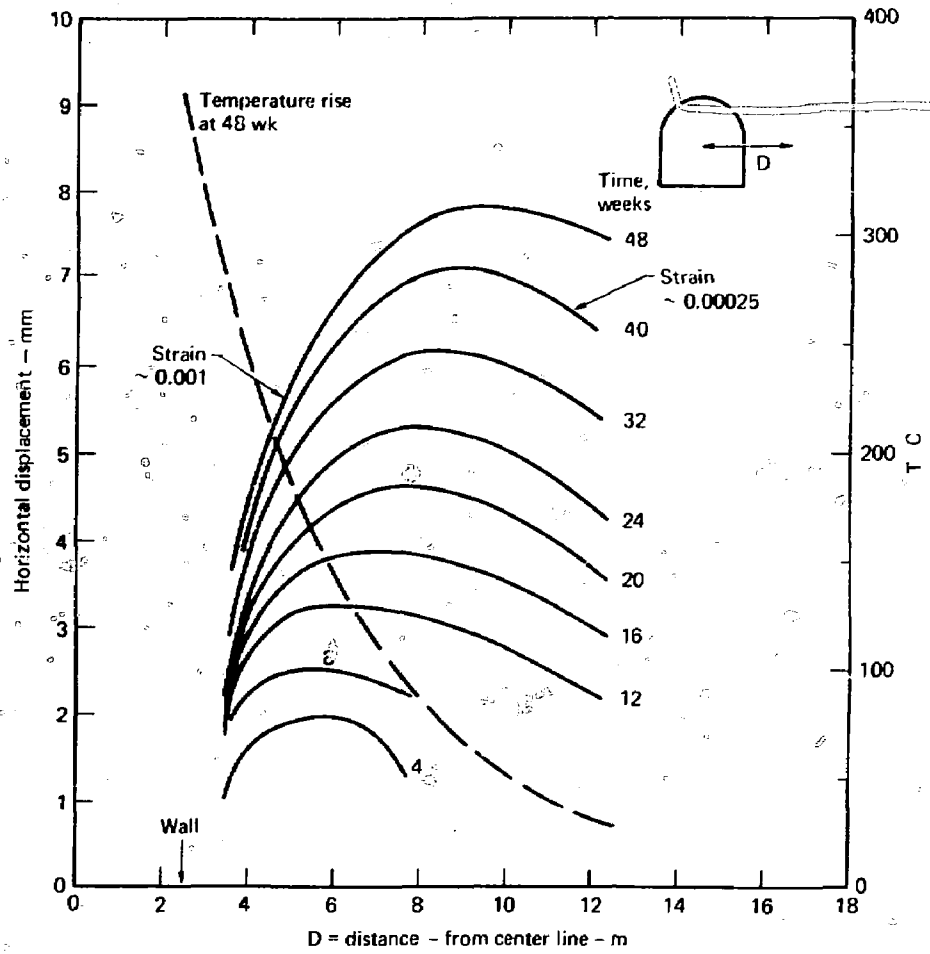

Fig. 10. Calculated horizontal displacement (positive outward) at the midplane of a 5-m wide, 5-m high drift heated with floor heaters with output of 5 kw/m of length. Displacement shown as a function of distance from drift centerline for several times, and temperature is shown at 48 weeks. Calculation, by LLL, is thermoelastic.

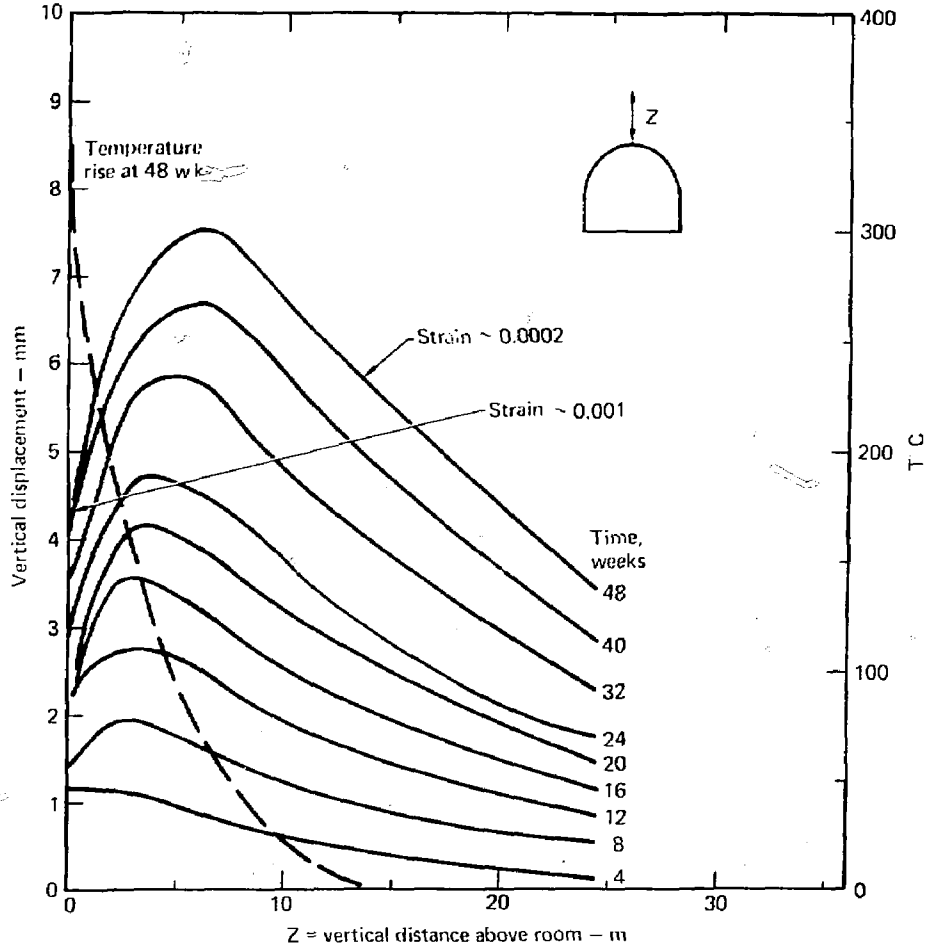

Fig.11. Calculated vertical displacement (positive up) directly above a 5-m wide, 5-m high drift heated with floor heaters with output of 5 kw/m of length. Displacement shown as a function of distance from roof for several times and temperature is shown at 48 weeks. Calculation, by LLL, is thermoelastic.

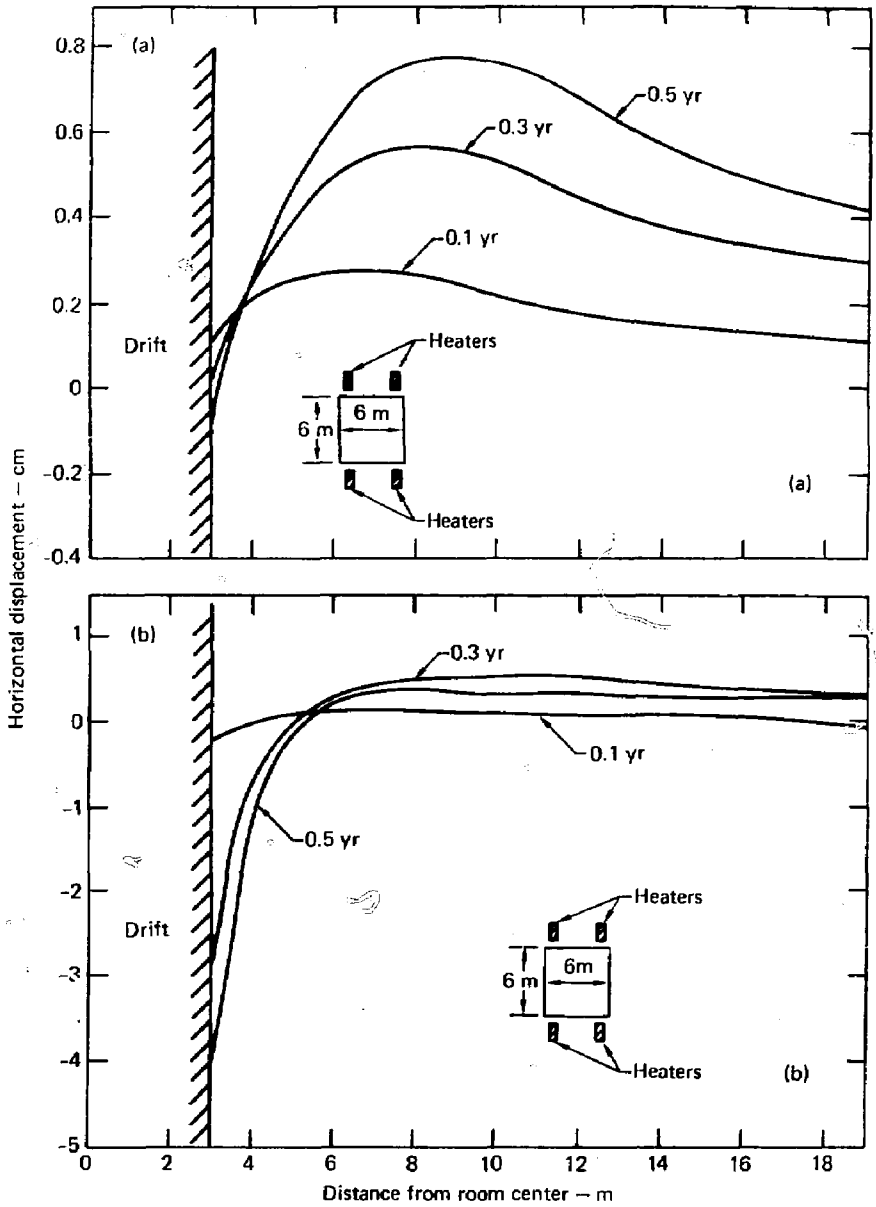

Fig. 12. Calculated horizontal displacement (positive out) along the midplane of a 6-m wide, 6-m high drift heated with 8 kw/m by heaters embedded as shown in the insert. Displacement shown as a function of distance from drift centerline for several times. Calculations, by RE/SPEC, are (a) thermoelastic and (b) allow failure.

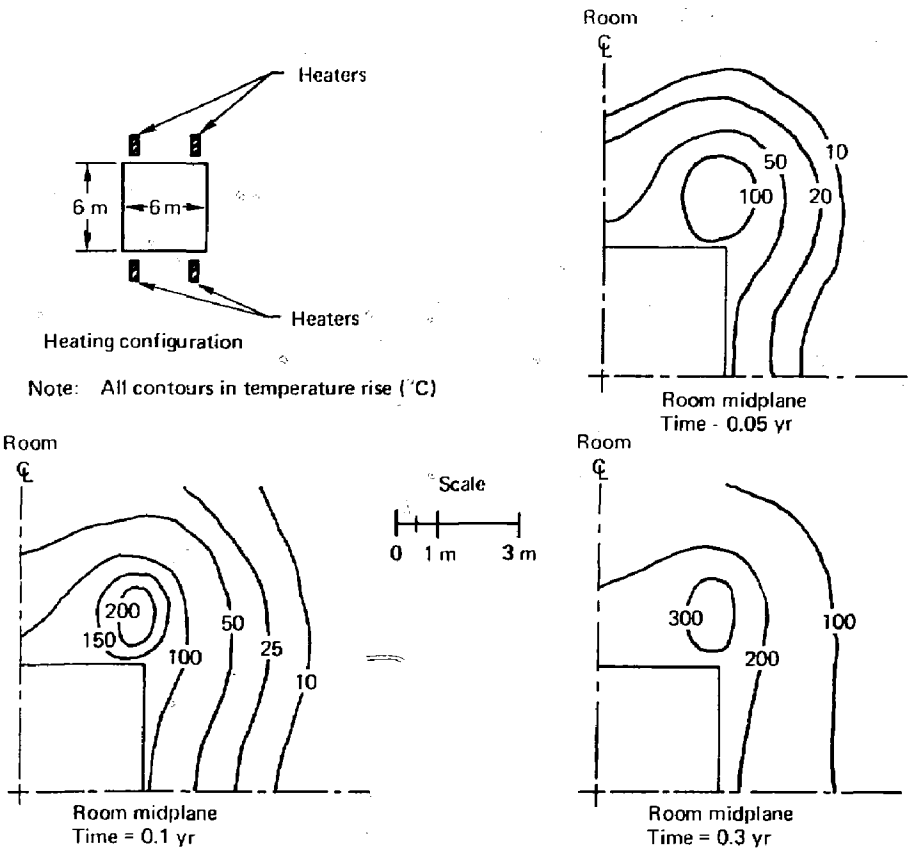

Fig. 13. Isotherms at three times for the calculation of a 6-m wide, 6-m high room heated with a 8 kw/m by heaters embedded as shown in the insert. Calculation by RE/SPEC.

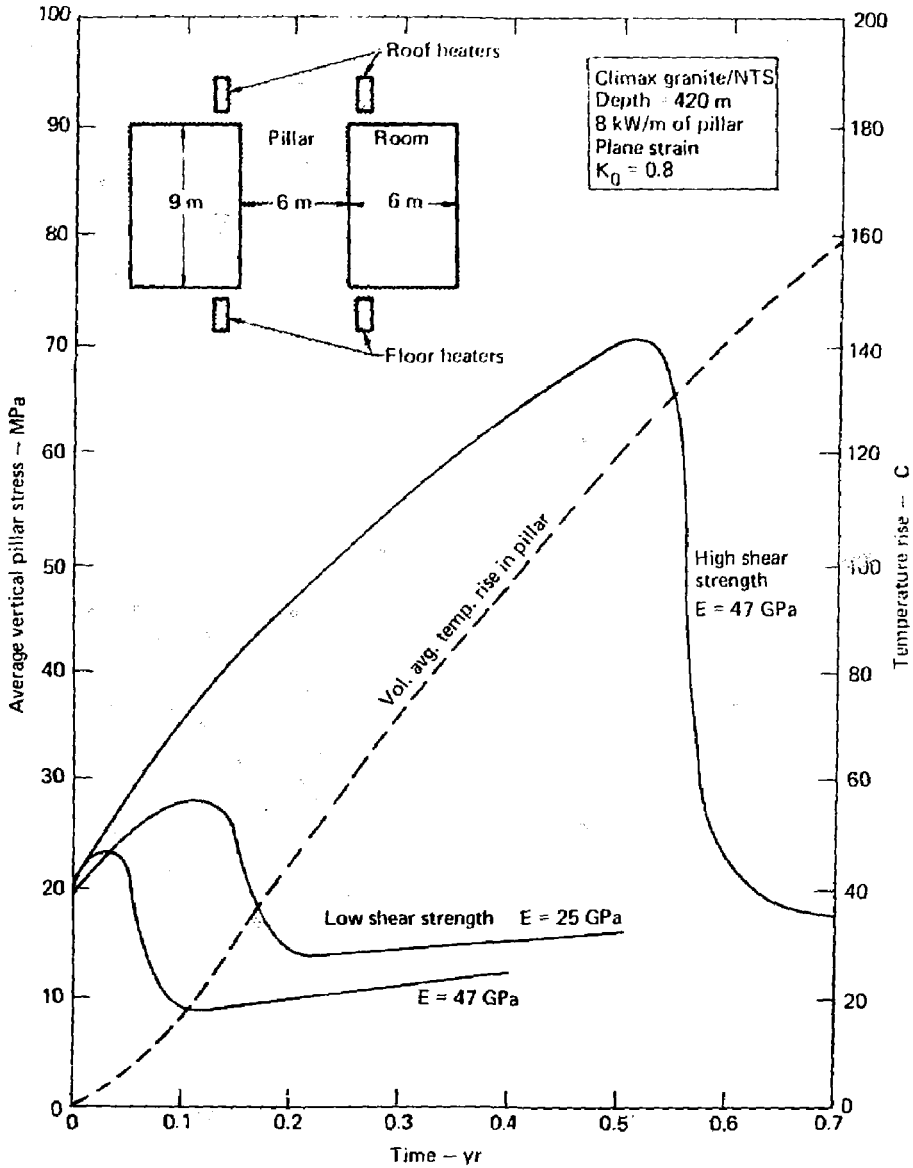

Fig. 14. Calculated volumetric average stress (compression positive) and temperature rise in a 6-m wide, 9-m high pillar between two drifts of the same size. Heat load was 8 kW/m of pillar from heaters as shown in the insert. Shear strengths of 13.8 MPa (50% strength) and 6.9 MPa (25% strength) were used. Young's moduli of 25 and 47 GPa were used in different runs. Calculation is by RE/SPEC.

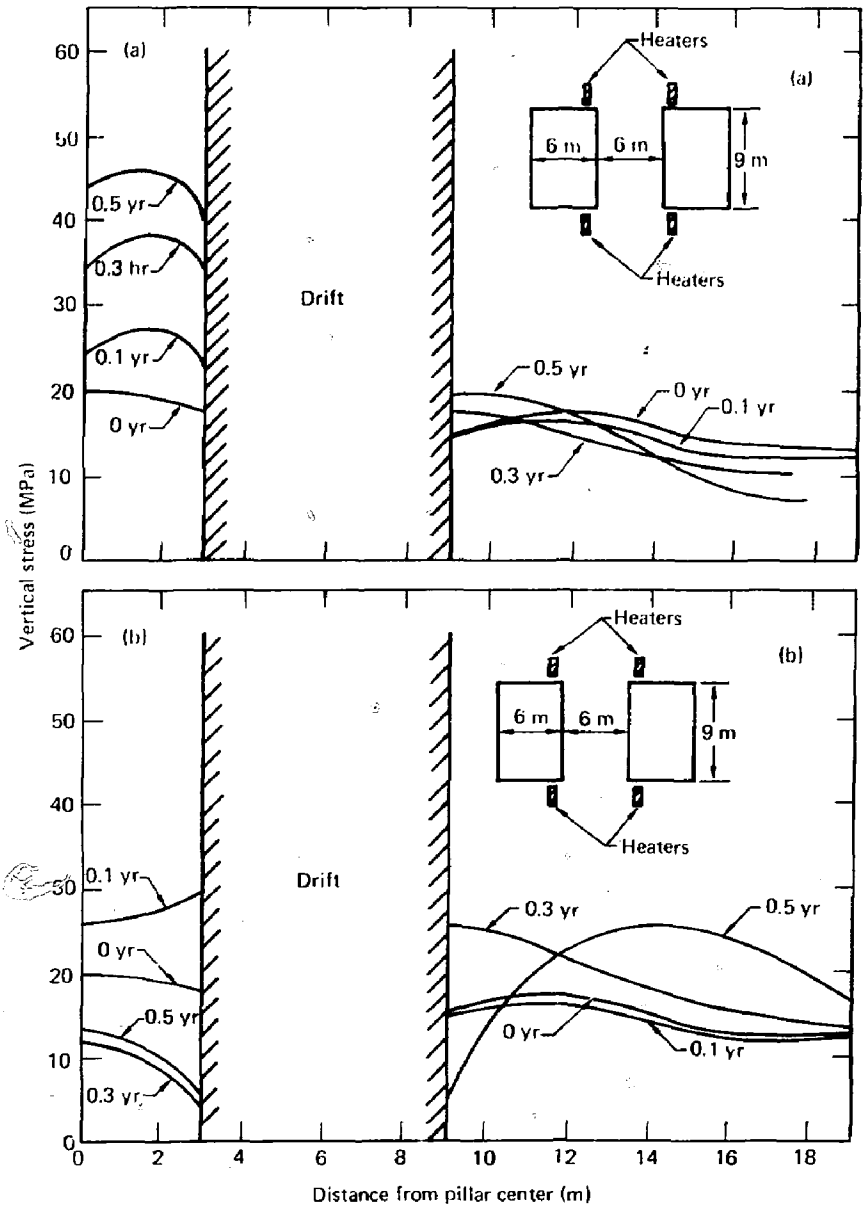

Fig. 15. Calculated vertical stress (compression positive) along the midplane of a problem consisting of a 6-m wide, 9-m high pillar between two 6-m wide, 9-m high drifts. Heat load was 8 kw/m supplied by heaters inserted as shown in the inset. Stress is shown at several times. The left boundary of the figure is the vertical center plane of the pillar. The blank area at the left center is the drift. The right half of the figure is the rib or wall of the drift on the opposite side from the pillar. Calculations, by RE/SPEC are (a) thermoelastic and (b) allow failure.

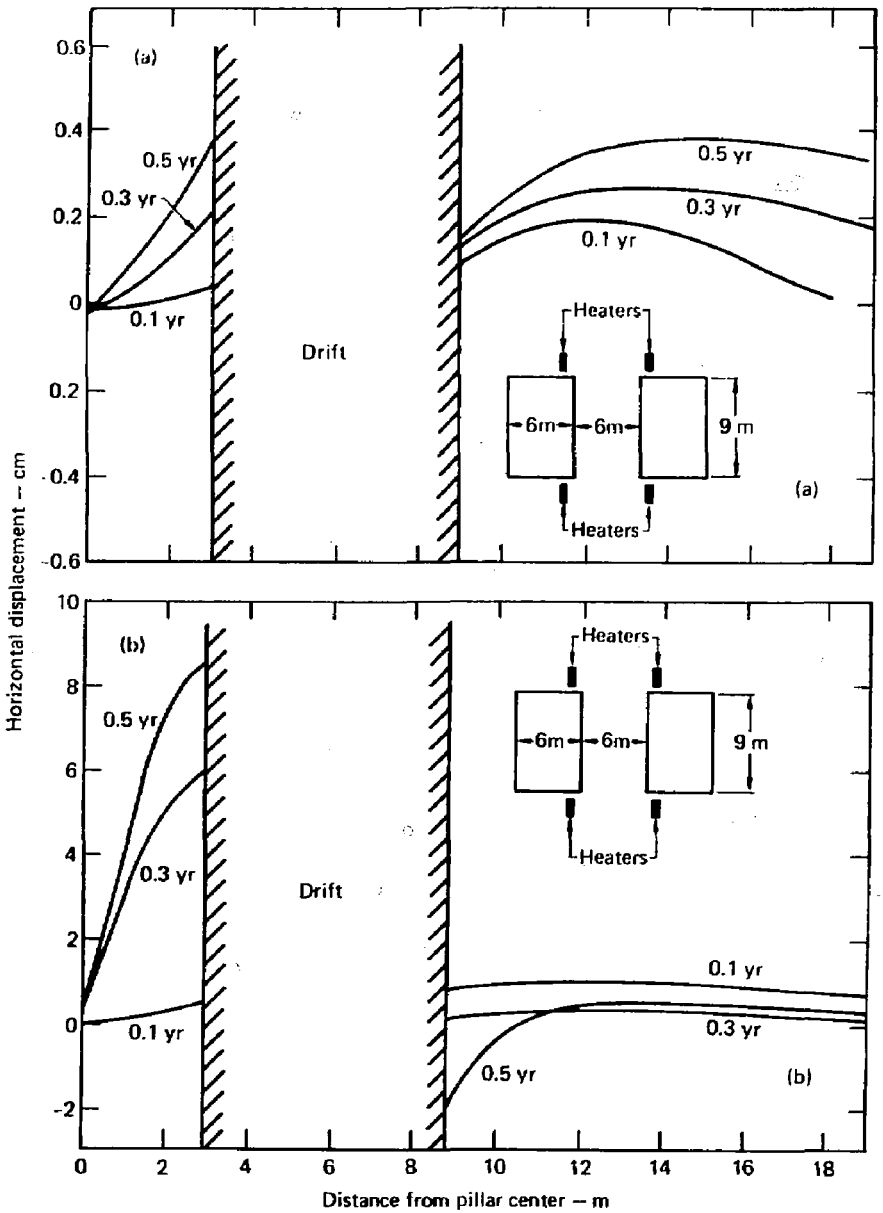

Fig. 16. Calculated horizontal displacement (positive out) along the midplane of a problem consisting of a 6-m wide, 9-m high pillar between two 6-m wide, 9-m high drifts. Heat load was 8 kw/m of pillar supplied by heaters inserted as shown in the inset. Displacement is shown at several times. The left boundary of the figure is the vertical center plane of the pillar. The blank area at the left center is the drift. The right half of the figure is the rib or wall of the drift on the opposite side from the pillar. Calculations, by RE/SPEC are (a) thermoelastic and (b) allow failure.

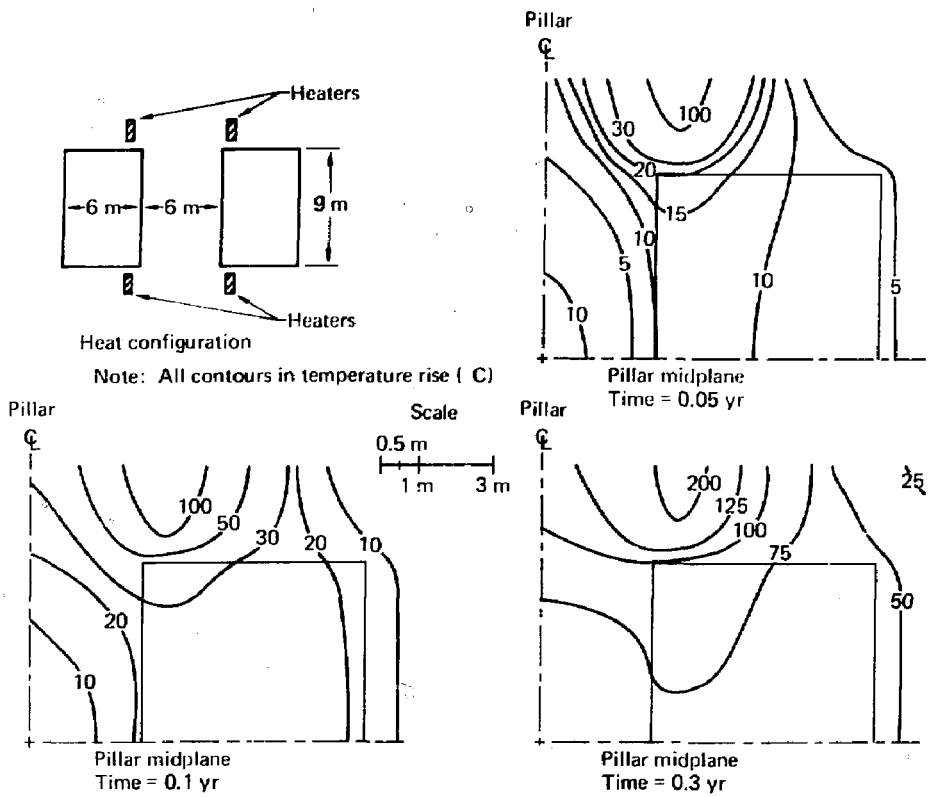

Fig. 17. Isotherms for the problem consisting of a 6-m wide, 9-m high pillar between two 6-m, 9-m high drifts. Heat load was 8 kw/m supplied by heaters as shown in the inset. Calculation by RE/SPEC.

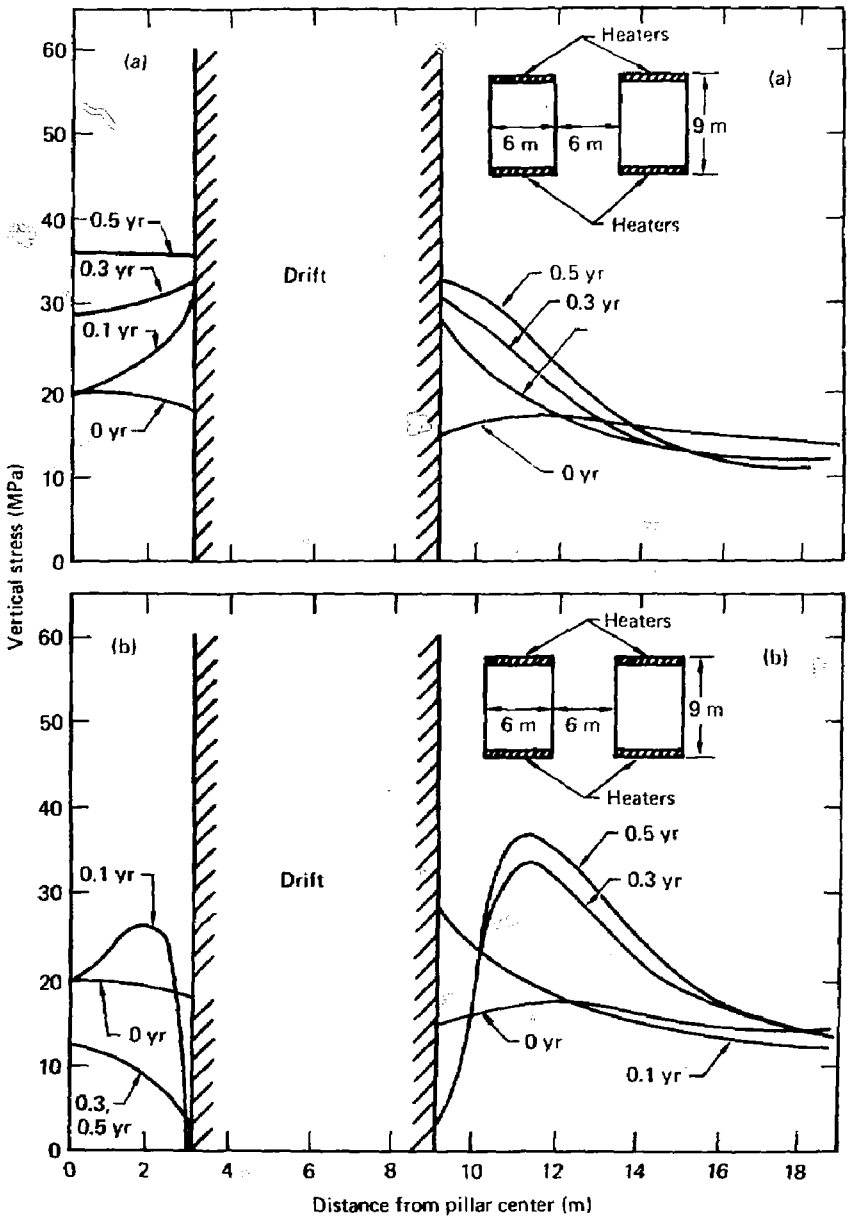

Fig. 18. Calculated vertical stress (compression positive) along the midplane of a problem consisting of a 6-m wide, 9-m high pillar between two 6-m wide, 9-m high drifts. Heat load of 8 kw/m was supplied by floor and roof heaters as shown in the inset. Stress is shown at several times. The left boundary of the figure is the vertical center plane of the pillar. The blank area at the left center is the drift. The right half of the figure is the rib or wall of the drift on the opposite side from the pillar. Calculations, by RE/SPEC are (a) thermoelastic and (b) allow failure.

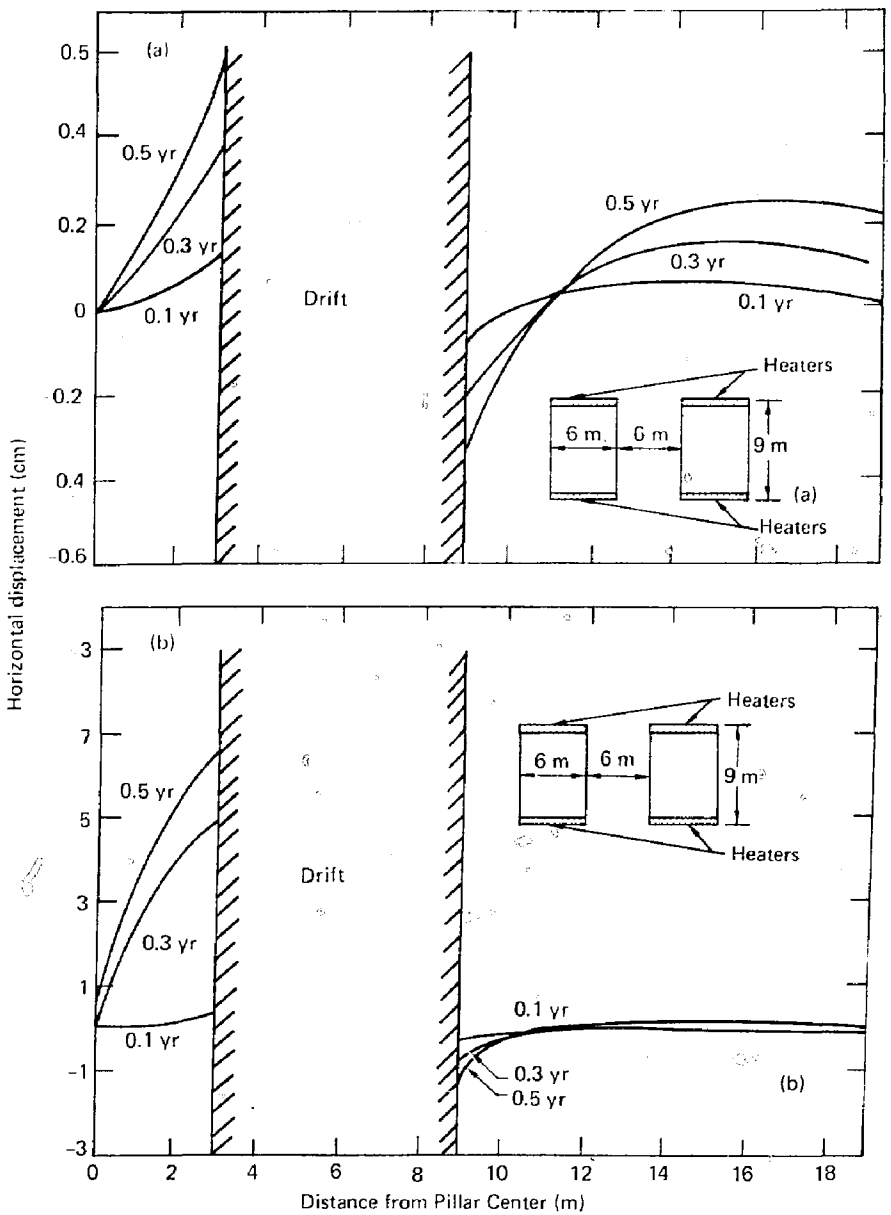

Fig. 19. Calculated horizontal displacement (positive out) along the midplane of a problem consisting of a 6-m wide, 9-m high pillar between two 6-m wide, 9-m high drifts. Heat load of 8 kw/m was supplied by floor and roof heaters as shown in the inset. Displacement is shown at several times. The left boundary of the figure is the vertical center plane of the pillar. The blank area at the left center is the drift. The right half of the figure is the rib or wall of the drift on the opposite side from the pillar. Calculations, by RE/SPEC are (a) thermoelastic and (b) allow failure.

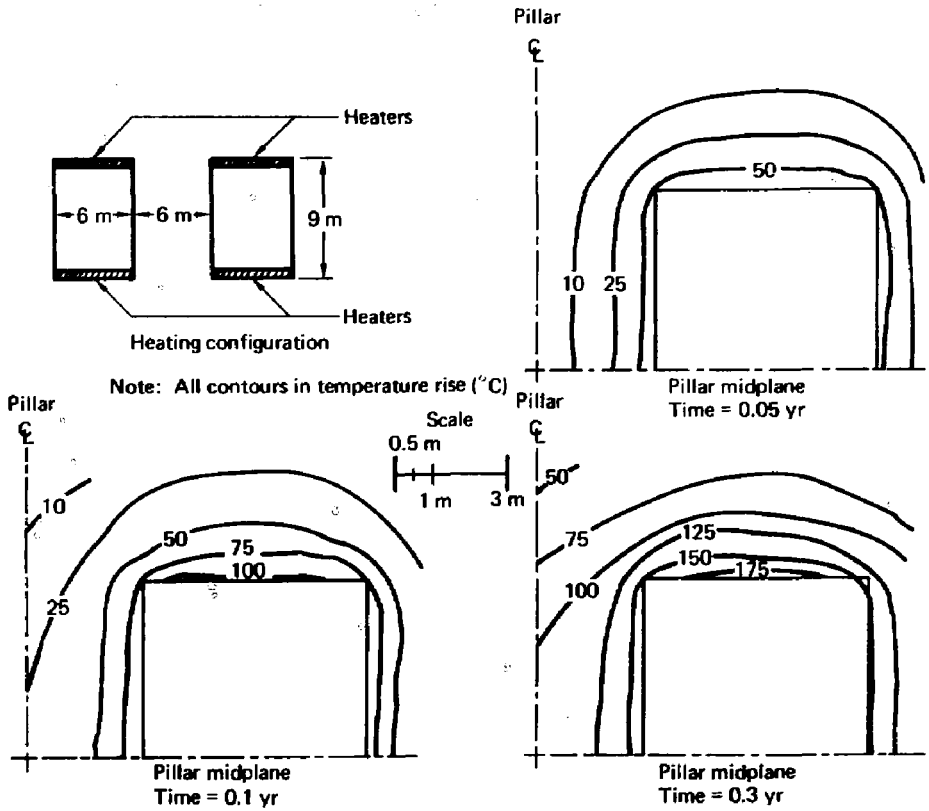

Fig. 20. Isotherms for the problem consisting of a 6-m wide, 9-m high pillar between two 6-m wide, 9-m drifts. Heat load was 8 kw/m supplied by roof and floor heaters as shown in the inset. Calculation by RE/SPEC.

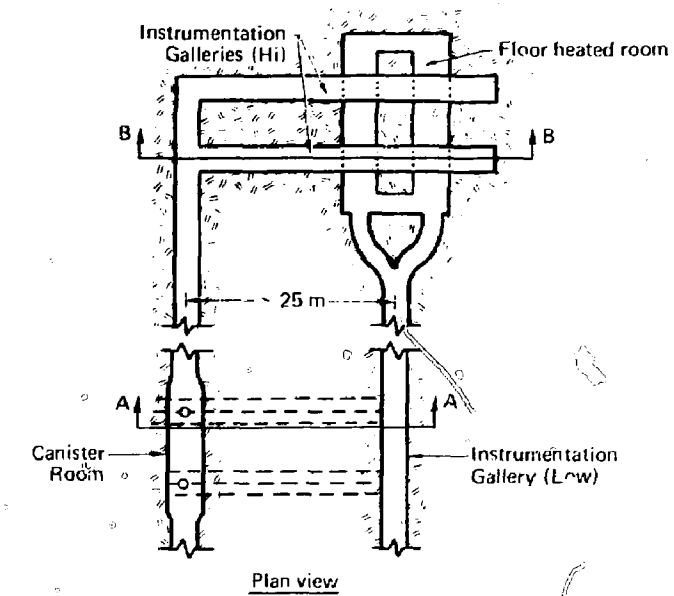

Fig. 21a

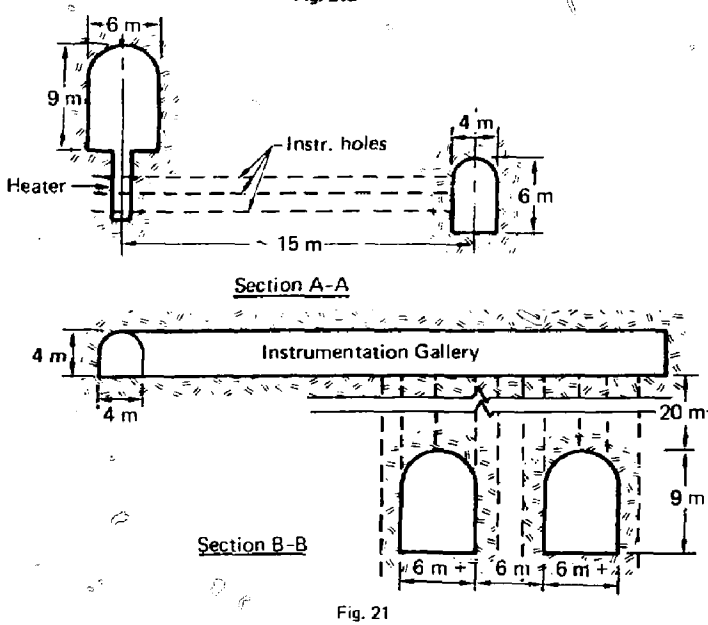

Fig. 21

Fig. 21. Plan (21a) and Section (21b) illustration of the design of the drifts for the two single-hole and two drift-and-pillar experiments. Instrument holes are shown as dashed lines.

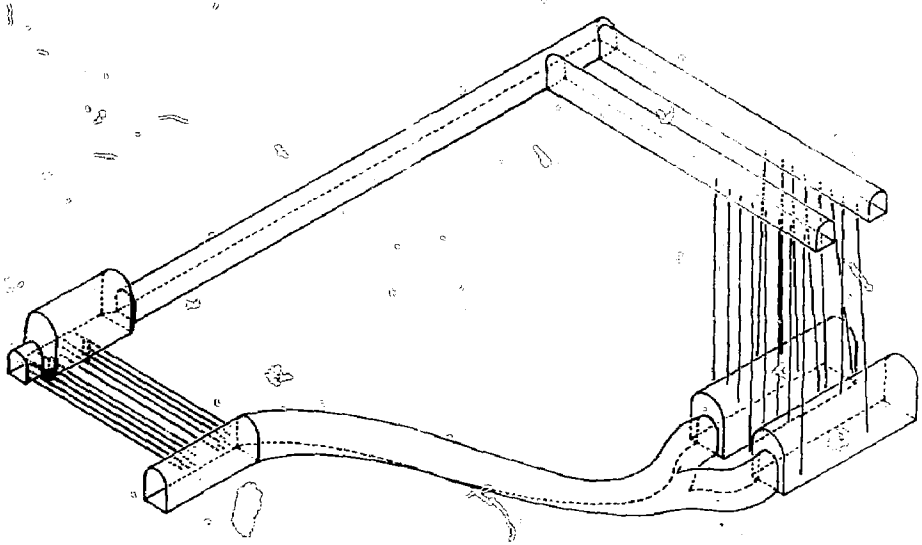

Fig. 21c

Fig. 21c. Isometric illustration of the design of the drifts for the two single-hole and two drift-and-pillar experiments. Instrument holes are shown as single lines.

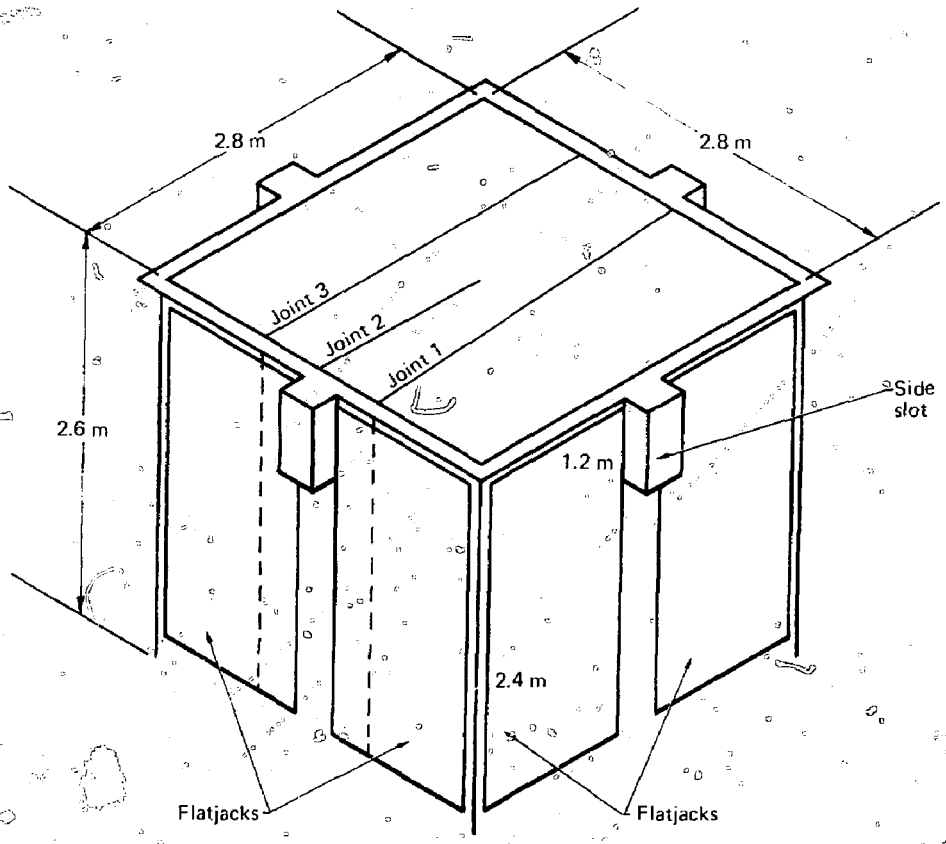

Fig. 22. Illustration of a flatjack experiment to measure *in situ* rock properties as a function of temperature and pressure.[15]

APPENDIX A

HOLOGRAPHIC INTERFEROMETRY: MEASUREMENT TECHNIQUE BY COINCIDENT ILLUMINATION AND VIEWING HOLOGRAPHIC INTERFEROMETRY (CIVHI)

H. Spetzler, CIRES, University of Colorado

Introduction

Topographic maps of the deformation of a surface may be obtained with optic holography (such as shown in Fig. 1). The contour interval is about 0.3 μm. Over a distance of several centimeters, the sensitivity of holographic interferometry is approximately the same as that of sensitive strain gauges. Over longer distances, the sensitivity of holography increases linearly with length.

The advantages of optical holography over other techniques are twofold:

1. The object to be investigated is in its own reference, which greatly reduces the usual problems associated with instrument drift and creeping of strain gauge backings.
2. The total visible surface becomes a gauge and subtleties in surface deformation due to preexisting flaws, such as joints, become readily apparent.

Resistance strain gauges and capacitive and magnetic devices are more portable and can more easily be adapted to a digital data handling system. The data obtained by holography are in quasi-digital form, where one fringe represents one bit. So much information is contained in topographic maps such as those shown in fig. 1 that the difficulty in digitization becomes one of selecting the most important part of the data. That most important part of

the data might easily be missed when gauges (e.g., resistance strain gauges) are used that simply average over their length.

General Information

Using laser-light, a three dimensional image of an object can be stored on a photographic plate - a hologram. When such an image is viewed, it is optically equivalent to looking through a window (the photographic plate upon which the image is stored) at the laser-light illuminated object. It is impossible, by passive optical means, to distinguish the real object from its image. If both the real object and its image coexist at the same place, and one, usually the object, becomes distorted, the light reaching the observer from the image interferes with the light from the object. The observer sees the object with superimposed black lines, interference fringes, which result when the two light paths are different by odd multiples of half of the optical wavelength. A permanent record of the distortion of the object may be obtained if the observer is a television or movie camera. In real time, the evolution of the fringes may of course be observed directly by eye or via a television monitor. By recording two images of the same object on one photographic plate, the difference between the images results in interference fringes which can be seen when viewing the developed plate in laser light.

A simple method for obtaining and interpreting deformation maps (interference fringes superimposed upon the object) has been developed. The object is illuminated by collimated parallel laser light from the same direction from which it is being viewed. The resultant deformation maps are insensitive to small (several wavelengths of light) rigid body translations and record only rigid body rotation and surface deformation. Pure rotation is readily recognizable since it produces only evenly spaced straight fringes, all parallel to

the axis of rotation. The angle γ through which an object is rotated is simply related to the fringe density m (i.e., number of fringes per cm) such that

$$\gamma = \sin^{-1} \frac{m}{2},$$

where λ is the wavelength of the laser light that is used to illuminate the object.

Surface deformation produces a deformation map, a topographic map where the fringes are the contour lines and the contour interval is equal to $\lambda/2$. It is important to emphasize that the deformation map is not a topographic map of the surface, but rather a map showing the deformation of the surface in the direction of observation. Only the relative displacement in the viewing direction causes fringes.

Examples

To illustrate these points, let us imagine a thermally expanding rectangular box. Let us assume that the linear coefficient of thermal expansion, α, is $5 \times 10^{-6}/°K$ and is the same in all directions, i.e., α is isotropic.

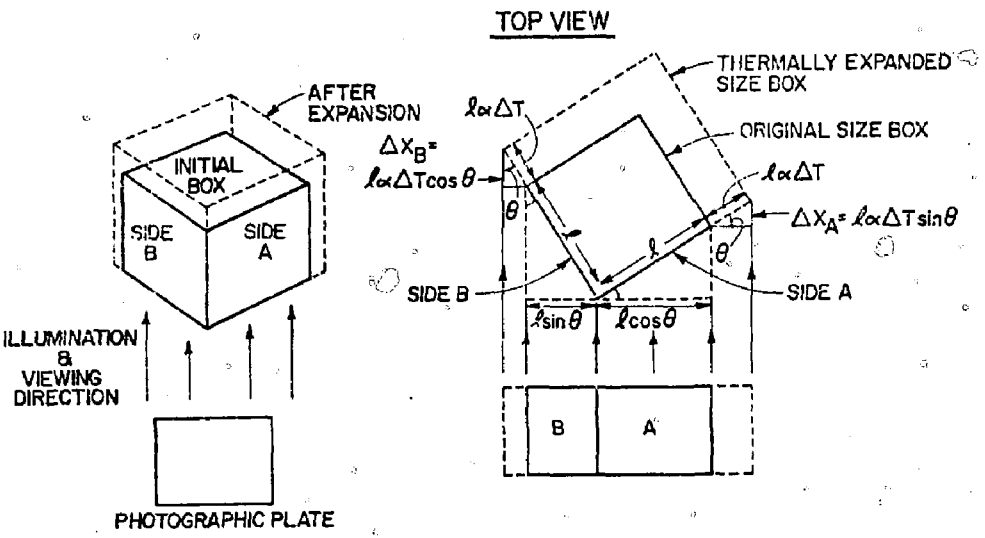

Fringe density Side B	Fringe density Side A
$M_B = \frac{2\Delta x_B}{\lambda \ell \sin \theta}$	$M_A = \frac{2\Delta x_A}{\lambda \ell \cos \theta}$
$M_B = \frac{2\ell\alpha\Delta T \cos \theta}{\lambda \ell \sin \theta}$	$M_A = \frac{2\ell\alpha\Delta T \sin \theta}{\lambda \ell \cos \theta}$
$M_B = \frac{2\alpha\Delta T}{\lambda} \cot \theta$	$M_A = \frac{2\alpha\Delta T}{\lambda} \tan \theta$

B. Numerical example: Box with a side length of 5 cm, viewed such that $\theta = 30°$, $\lambda = 0.63\mu$, $\alpha = 5 \times 10^{-6}/°K$, $\Delta T = 20°K$.

On side A there will be

$$M_A = \frac{2 \tan 30° \times 5 \times 10^{-6} \times 20}{0.63 \times 10^{-4} \text{ cm}} = 1.83 \text{ fringes/cm}$$

On side B there will be

$$M_B = \frac{2 \cot 30° \times 5 \times 10^{-6} \times 20}{0.63 \times 10^{-4} \text{ cm}} = 5.50 \text{ fringes/cm}$$

The total number of fringes on each side amounts to the projected width of the side times the fringe density.

For side A $\ell \cos \theta \times 1.83 = 7.92$ fringes

For side B $\ell \sin \theta \times 5.50 = 13.75$ fringes

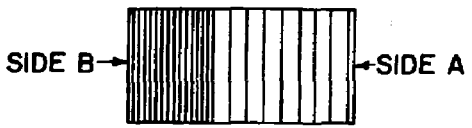

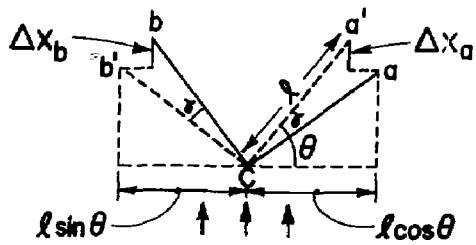

Let us consider a small amount of rotation of the above box:

Point "a" moves back a distance

$$\Delta x_a = 2\ell \sin \gamma/2 \cos (\theta + \gamma/2)$$

Point "b" moves forward a distance

$$\Delta x_b = 2\ell \sin \gamma/2 \sin (\theta + \gamma/2)$$

The fringe density on side A will be

$$\frac{2\Delta x_a}{\lambda\, \ell \cos \theta} = \frac{4\ell \sin \gamma/2 \cos (\theta + \gamma/2)}{\lambda\, \ell \cos \theta}$$

and on side B will be

$$\frac{2\Delta x_b}{\lambda\, \ell \sin \theta} = \frac{4\ell \sin \gamma/2 \sin (\theta + \gamma/2)}{\lambda\, \ell \sin \theta}$$

but for small rotations, i.e., small γ

$$2 \sin \gamma/2 \approx \sin \gamma$$

and $\cos (\theta + \gamma/2) \approx \cos \theta$; $\sin (\theta + \gamma/2) \approx \sin \theta$; therefore, the fringe density, m, for both sides due to a rotation of angle γ is $\frac{2 \sin \gamma}{\lambda}$.

A rotation of 1.57×10^{-4} radians gives a fringe density of 5 fringes/cm.

It is important to realize that the information contained in a deformation map is ambiguous as to the sign of surface deformation or rotation. Two optical images are interfering and no information is contained in the deformation

map as to which image came first. If some knowledge of the sense of deformation or rotation is available, this ambiguity can be removed. For example, during a thermal expansion measurement, if it is known that the temperature is increasing between the recording of the two images, and that the coefficient of thermal expansion is positive, there is no problem with interpretation. If it is necessary to obtain the sense of deformation, it is often useful to intentionally add deformation or rotation of a known amount and direction. To understand this numerically, let us use the box of the previous examples.

This time, between the recording of the two images, we will have intentionally added the rotation corresponding to 5 fringes/cm in the counterclockwise direction. We also have experienced a 20°K temperature rise between the recording of the two images. The deformation map will now tell us if the box expanded or contracted.

During counterclockwise rotation, point a moved further away from the observer with respect to point c, while point b came closer. During expansion of the box, both points a and b moved further away with respect to point c. The sense of motion for expansion and rotation on face A is the same and the fringe densities are additive. On face B the rotation brought point b closer and expansion moved it further away, resulting in a fringe density which is the difference between the two individual ones. Although on the hologram we cannot determine positive fringes, let us define relative motion away from the observer to add positive fringes to the deformation map and vise versa for relative motion toward the observer. The counterclockwise rotation will then end up with a positive rotation fringe density M_R on face A and a negative fringe density $-M_R$ on face B.

For thermal expansion and counterclockwise rotation we have the total fringe density on face A

$$A = M_A + M_R = 1.83 + 5 = |6.83| = 6.83$$

and on B

$$B = M_B - M_R = 5.5 - 5 = |0.5| = 0.5$$

Similarly, for thermal contraction

$$A = -M_A + M_R = -1.83 + 5 = |3.17| = 3.17$$

$$B = -M_B - M_R = -5.5 - 5 = |-10.5| = 10.5$$

Since the final fringe density is only a number, we must take the absolute values.

Now let us do the problem in reverse, knowing that we introduced counterclockwise rotation of 5 fringes.

Case 1. The fringe densities observed on each face are:

$$A = 6.83$$

$$B = 0.5$$

$$\frac{M_A}{M_B} = \frac{2 \tan \theta\, \alpha\Delta T}{2 \cot \theta\, \alpha\Delta T} = \tan^2 \theta \quad \text{but } \theta = 30°$$

$$\frac{M_A}{M_B} = \frac{1}{3}$$

First assume that A and B are both positive:

$$M_A + M_R = 6.83 = M_A + 5 = 6.83 \quad \Big| \quad M_A = 1.83$$

$$M_B - M_R = 0.5 = 3M_A - 5 = 0.5 \quad \Big| \quad M_A = 1.83$$

If we had assumed:

A = positive $M_A + 5 = 6.83$ $M_A = 1.83$

B = negative $3M_A - 5 = -0.5$ $M_A = 1.5$

which is incompatible

Assume contraction, i.e., negative M_A

A = negative $\quad M_A + 5 = -6.83 \quad M_A = -11.83$

B = neg or pos $\quad 3M_A - 5 = \pm 0.5 \quad M_A$ can only be positive

Therefore Case I must correspond to expansion.

Case II. The fringe densities on each face are:

$$A = 3.17$$

$$B = 10.5$$

First assume expansion.

$M_A + 5 = \pm 3.17$ implies M_A = negative

B = pos $3M_A - 5 = 10.5 \quad M_A = 5.16$ incompatible

Expansion is not possible since there is no possible answer for A where M_A is positive.

Now assume contraction

both negative $\quad M_A + 5 = -3.17 \quad M_A = -8.17$

$3M_A - 5 = -10.5 \quad M_A = 1.83$ incompatible

A positive $\quad M_A + 5 = 3.17 \quad M_A = -1.83$

B negative $\quad 3M_A - 5 = -10.5 \quad M_A = -1.83$ compatible

Therefore Case II corresponds to contraction.

Gauge Sensitivity

The number of fringes, n, produced by a differential displacement, Δx, is

$$n = \frac{2\Delta x}{\lambda}$$

For practical purposes, we may not wish to interpolate to closer than 0.1 fringes. The sensitivity, $\frac{\Delta x}{\ell}$, is then $\frac{n\lambda}{2\ell}$; if n = .1,

$$\frac{\Delta x}{\ell} = \frac{\lambda}{2D}$$

For typical laser light, e.g., HeNe with λ = .63 μm and the dimensions of an instrument hole with a diameter of 5 cm

$$\frac{\Delta x}{\ell} = \frac{.6 \times 10^{-4}}{100} = 10^{-6}$$

Therefore the maximum practical sensitivity, where the diameter of an instrument hole is concerned, corresponds to a strain of 10^{-6} cm/cm or a rotation of 10^{-6} radians.

In the case of a hologram where an entire wall or floor is concerned, of linear dimensions of say 3 meters, the corresponding sensitivity would be

$$\frac{\Delta x}{\ell} = \frac{.6 \times 100^{-4}}{60 \times 100} = 10^{-8}$$

A practical gauge

The radial expansion and tilt of an instrumentation hole can readily be measured by a triangular gauge constructed from two rigid rectangular strips of a suitable material hinged as shown.

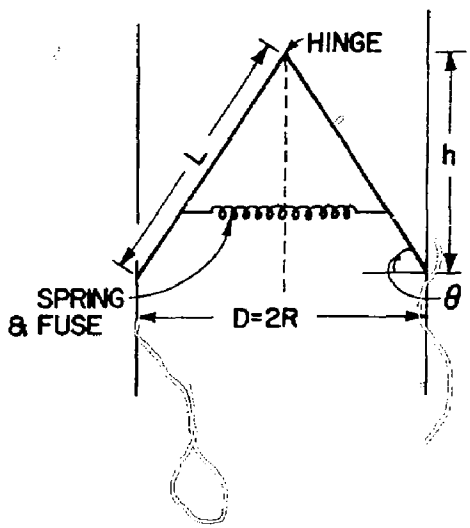

The spring between the metal strips is initially held compressed by an easily burned fuse wire; the gauge is lowered into position and the fuse wire burned to release the spring, which then forces the metal strips against the sides of the hole. This spring may be either a coil or a leaf spring.

The sensitivity of the gauge is determined by the ratio of the gauge length to the radius of the hole. Since a change in h produces the fringes, let's define the sensitivity of the gauge as $\frac{dh}{dR}$.

$$h^2 = L^2 - R^2$$

$$\frac{dh}{dR} = -\frac{R}{h} = -\cot \theta$$

As the hole expands h decreases and vise versa. A sensitivity of one is achieved when $\theta = 45°$ and $L = \sqrt{2}R$. An amplification by a factor of 2 is achieved when $\theta = 26.57°$ and $L = 1.118R$ and an attenuation by a factor of 2 when $\theta = 63.43°$ and $L = 2.236R$.

A view down hole with six installed gauges is shown below. Each is 3/8" wise and touches the circumference of the hole at three points.

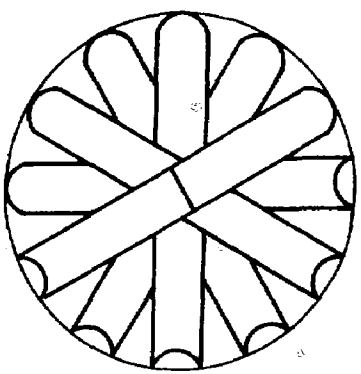

If it is desirable to increase the number of gauges per hole, the width of each gauge may be reduced and/or one of the strips may be replaced by a thin rod. When implacing the gauges, the bottom-most gauge must be positioned first; a stiff tube with some electrical wires (to burn off the fuse wire) can be used as an implacement tool.

Once the gauges are implaced, a periodic check as to the sensitivity and stability of the active optical and readout system may be desirable. This can be accomplished in a number of different ways; one possibility is to introduce intentional rotation into the reference beam system and thus produce fringes. It may be preferable, however, to introduce a transient fringe pattern on gauges perhaps by heating them with a light source. If the gauge material were chosen to have a positive thermal expansion coefficient of $5 \times 10^{-6}/°C$, a 6°C temperature rise would add or subtract one fringe per cm depending whether the hole is in a stage of contraction or expansion respectively. If we assume a gauge size of 8.8 cm x 1 cm x .1 cm (amplification factor one), a heat capacity of the gauge material of 0.5 cal/cm^3, an emissivity of the gauge material of 0.5 and a minimum projected exposed gauge area of 3 cm^2, a light source that can deliver about 20 joules per gauge or 250 joules per hole per calibration is required. The light from a 100 watt light bulb focused into the hole for 2.5 sec would deliver enough energy. The time required for a gauge to reach thermal equilibrium upon irradiation should be on the order of the irradiation time and long with respect to its cooling time.

A workable optical system for an instrumentation hole

Any reasonable number (say 10 or 20) of instrumentation holes can be part of one optical system using one, or perhaps two lasers, where one serves as a back up. The sketch shows one such possible system.

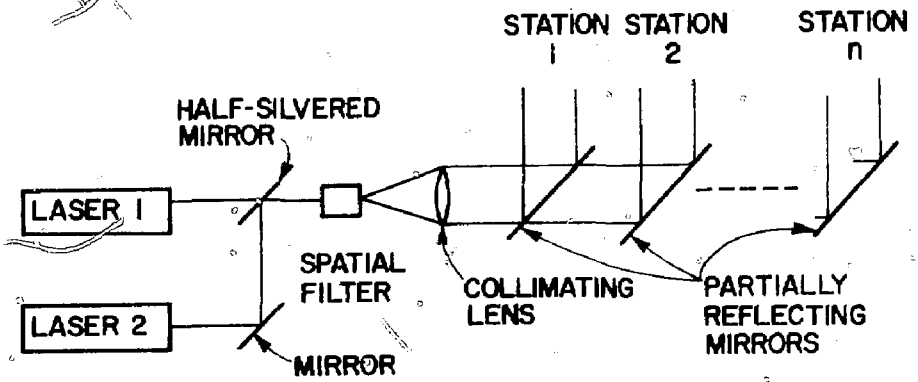

Lasers No. 1 and 2 can be used interchangeably. In our laboratory we have produced double exposure holograms with valid topographic maps by using an 18 mW and a 3 mW He-Ne laser for the first and second exposure respectively. Our exposure times using the 18 mW laser and a 10 cm diameter beam are between 2 and 5 seconds. For the measurements in the mine, ~500 mW Argon lasers (or similar units) would be used because of their longer coherence length. If ten instrumentation holes are to be measured, partially reflecting mirrors ranging from 10%, 11.1%, 12.5%. . .to 100% must be used to supply each hole with the same laser light intensity. The sketch of the holocamera shows all the functional components. The relative stability of the beam splitter and the subsequent components are critical. It is only the motion of these parts that contribute to fringe formation.

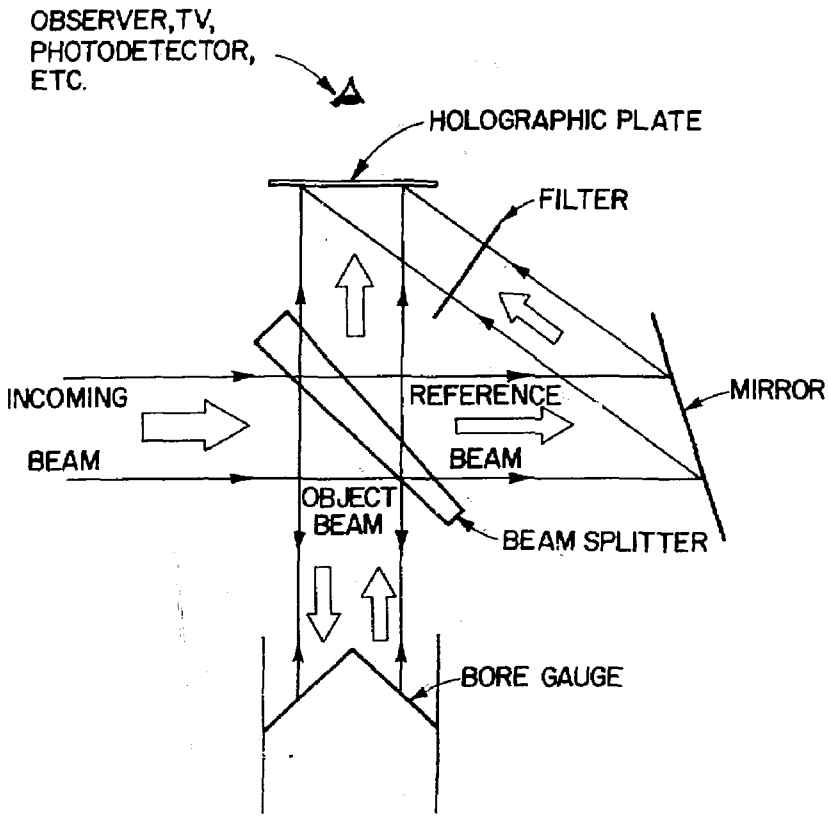

Data acquisition and dissemination system

One of the great advantages of the holographic interferometric system is the fact that it contains such a great amount of information. This advantage over other systems should not be discarded. The responsible scientist or engineer should always be able upon command to observe the fringe pattern. This

is especially important when pillar, mine wall, or floor deformations are being measured. As an illustration, see the attached photo of a double exposed hologram where a man touches and deforms a 9 feet diameter space antenna.

When digitization is desirable, it can readily be accomplished by fringe counting with a photosensitive device. It is best to use a pair of such devices to ascertain the direction of fringe motion as well as the fringe count. Since the change in fringe patterns will be very slow in the proposed heating (and real disposal) tests, it would be prudent to introduce an initial fringe pattern by pre-rotation and observe its changes. Continuous scanning of the fringe pattern will introduce the inherently greater sensitivity of an A.C. measurement over that of a D.C. measurement.

Especially useful will be a correlation of the deformation maps of boreholes and walls with other data obtained from microseismicity, acoustic velocity and spectrum changes, and especially infrared mapping when joints and pore fluids are involved.

Numerical example for 40 kw heated hole test

In this numerical example we use a gauge as described under "A practical gauge" with a sensitivity of one and a positive coefficient of thermal expansion of $5 \times 10^{-6}/°C$. Let the observation hole be 5 meters from the 40 kw heater hole. According to Figure 9, in 4 weeks the observation hole has moved 1.2 mm from the heater hole.

Taking the slope from fig. 9 the average differential rate of motion across the hole is $\frac{2mm}{3.2m}$ or 3.1×10^{-4} strain in 4 weeks. With a sensitivity of one this strain produces a fringe density of

$$\frac{3.1 \times 10^{-4}}{\lambda/2} = \frac{2 \times 3.1 \times 10^{-4}}{.6 \times 10^{-4}} \approx 10 \frac{\text{fringe}}{\text{cm}}$$

By introducing a pre-rotation we can readily resolve one tenth of one fringe and could therefore determine the strain in the hole diameter to one percent in 4 weeks. This strain is in the radial direction from the heated hole and is in response to compression, thus the gauge height is increasing.

After 8 weeks the hole will have moved a total of 1.9 mm relative to the heater hole and show 13.5 fringes. The main effect during the second and subsequent 4 week intervals is for the hole to move radially outward, and slowly warm up until well after one year the thermal wave catches up to the hole and it will expand instead of contract. It will take about 42 weeks until the hole will have heated 100°C above ambient and the thermal expansion of the gauge will have contributed 16.6 fringes/cm in the same sense as the strain of the hole. If the temperature is measured separately, it is easy to subtract the additional fringes. A gauge sensitivity of one and a thermal expansion coefficient α of 5×10^{-6} may then be appropriate. By using fused quartz for the gauge material, α can be reduced to 10^{-7}/°C and thermal fringes cease to be a problem. The system check out will then have to be based upon some other techniques such as induced rotation. Of course, not all gauges must have the same α or the same sensitivity. The variety is infinite and the possibilities only limited by the imagination of the designer. The attached figures show several examples of the use of holographic interferometry. Please see the figure captions for the explanations.

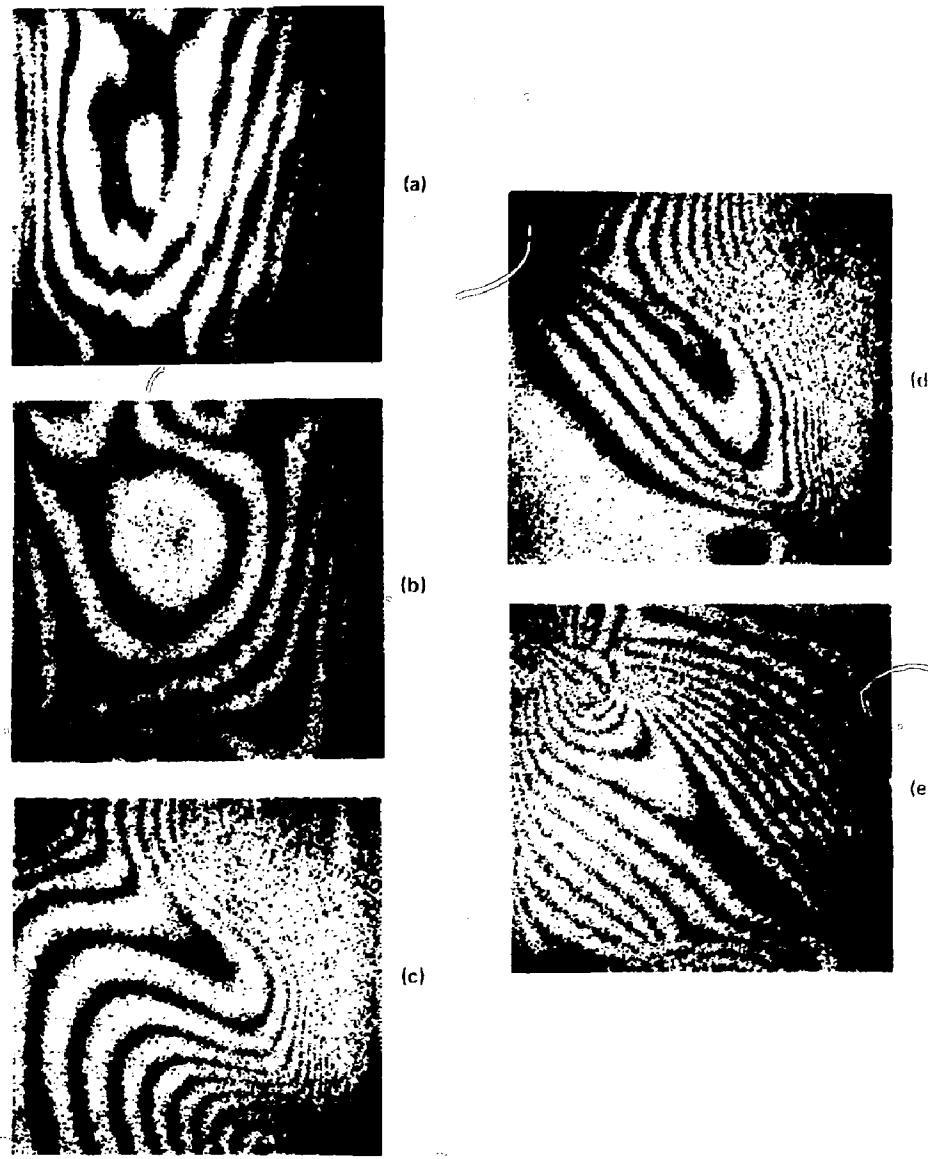

Fig. A1. A sequence of photographs of doubly exposed holograms is shown. The formation of an intense deformation zone is clearly visible between Figures 1b and 1d as the stress is increased from 50% to 84% of ultimate principal stress, σ_1. Figures 1a and 1e show the sample in its virgin state and after a macrofracture has started, respectively.

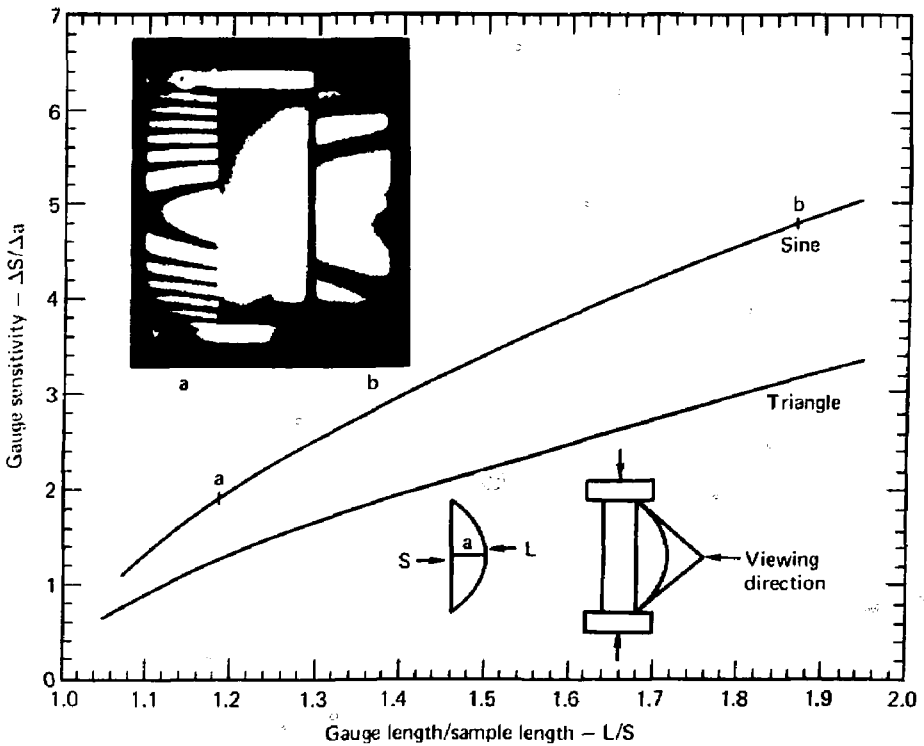

Fig. A2. Gauges similar to those suggested in the text are shown. The graph gives the gauge sensitivity versus gauge length to sample length ratio. The photo insert shows the response of two sinusoidal gauges to a nominal sample shortening of 3 μm. Sample length is 44 mm and gauge-length to sample-length ratios for a and b are 1.13 and 1.86, respectively. Non parallelism of fringes is the result of a tilt of less than 0.2 μm across the sample.

Fig. A3. A 3 meter diameter antenna is deformed by the touch of a finger. The fringes are a measure of the amount of deformation. A pulsed Ruby laser was used for the illumination because of its long coherence length.

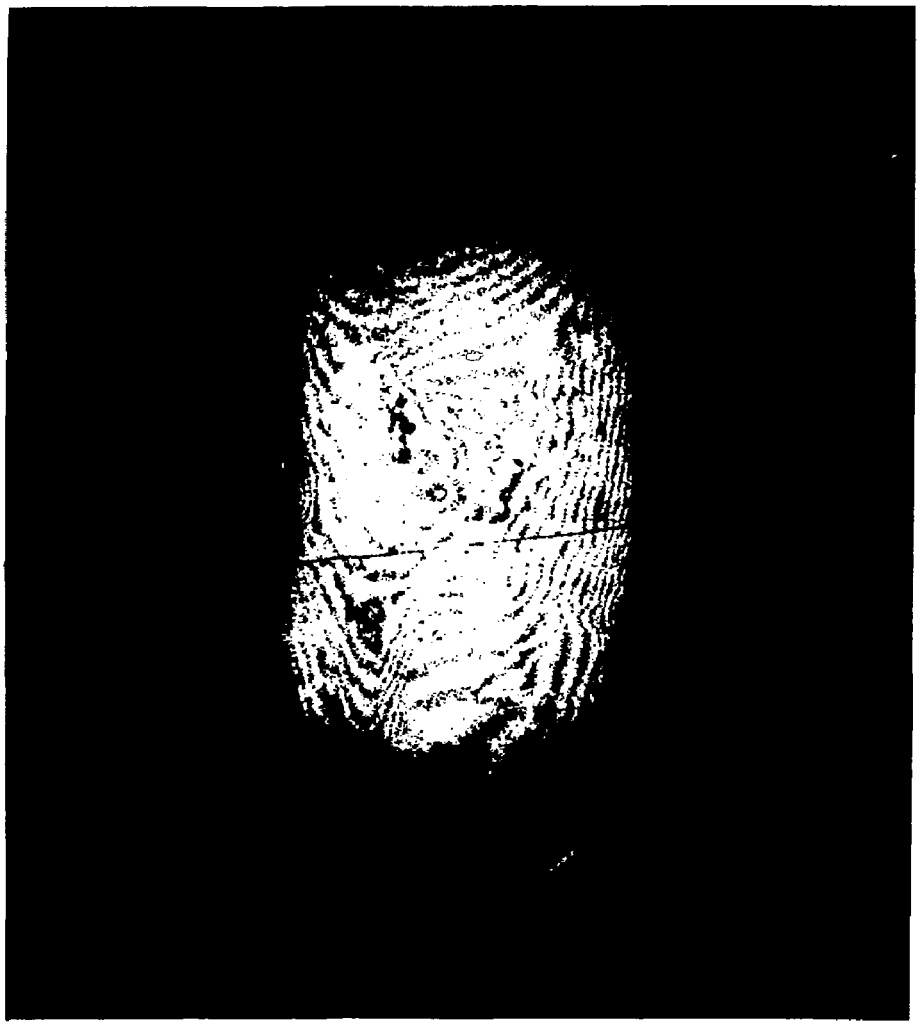

Fig. A4a. A temperature change of 15 Centigrade caused the deformation on this 5.2 cm diameter core from the Climax Stock. While the average coefficient of linear expansion is about 0.8×10^{-5}/ C, the actual coefficient varies by more than a factor of 2.

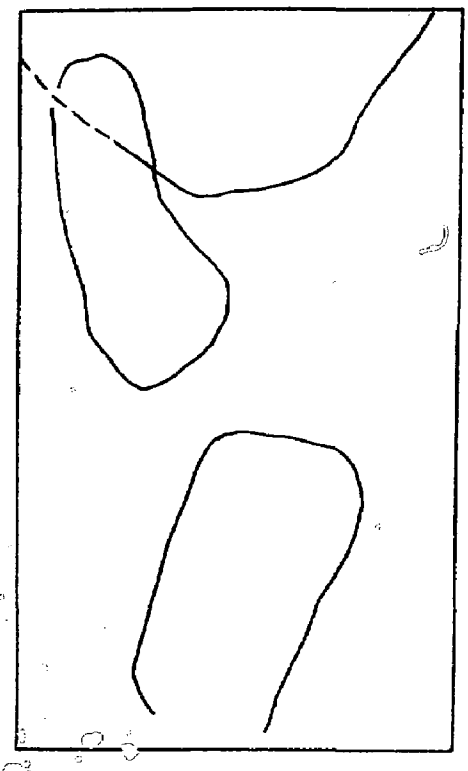

Fig. A4b. Shows the outline of the sample. The topmost trace is a healed fracture that is barely visible on the core *but for most of its trace visible as a feature where the fringes are discontinuous on the hologram. The two elongated* features are presumably phenocrysts. The lower one is visible on the surface, the upper one is beneath the surface. The crack is continuously visible on the sample but does not show up as a discontinuous feature on the hologram where it crosses the upper feature.